Journal of Geophysical Research: Oceans

RESEARCH ARTICLE
10.1029/2018JC014424

Ocean Circulation Causes Strong Variability in the Mid-Atlantic Bight Nitrogen Budget

Marjorie A. M. Friedrichs[1], Pierre St-Laurent[1], Yongjin Xiao[1], Eileen Hofmann[2], Kimberly Hyde[3], Antonio Mannino[4], Raymond G. Najjar[5], Diego A. Narváez[2,6], Sergio R. Signorini[7], Hanqin Tian[8], John Wilkin[9], Yuanzhi Yao[8], and Jianhong Xue[10]

[1]Virginia Institute of Marine Science, College of William & Mary, Gloucester Point, VA, USA, [2]Center for Coastal Physical Oceanography, Old Dominion University, Norfolk, VA, USA, [3]National Oceanic and Atmospheric Administration, National Marine Fisheries Service, Northeast Fisheries Science Center, Narragansett, RI, USA, [4]NASA Goddard Space Flight Center, Greenbelt, MD, USA, [5]Department of Meteorology and Atmospheric Science, The Pennsylvania State University, University Park, PA, USA, [6]Departamento de Oceanografía y Centro de Investigación Oceanográfica COPAS Sur-Austral, Universidad de Concepción, Concepción, Chile, [7]Science Applications International Corp., NASA Goddard Space Flight Center, Greenbelt, MD, USA, [8]School of Forestry and Wildlife Sciences, Auburn University, Auburn, AL, USA, [9]Department of Marine and Coastal Sciences, Rutgers, The State University of New Jersey, New Brunswick, NJ, USA, [10]Marine Science Institute, The University of Texas at Austin, Port Aransas, TX, USA

Key Points:
- A biogeochemical-circulation model is used to quantify the nitrogen budget of the Mid-Atlantic Bight (MAB)
- Horizontal along-shelf and across-shelf fluxes dominate the spatiotemporal variability of net community production (NCP) in the MAB
- Highest NCP is found in a year when inorganic nitrogen entering from across the continental slope is high and terrestrial inputs are low

Correspondence to:
M. A. M. Friedrichs,
marjy@vims.edu

Citation:
Friedrichs, M. A. M., St-Laurent, P., Xiao, Y., Hofmann, E., Hyde, K., Mannino, A., et al. (2019). Ocean circulation causes strong variability in the Mid-Atlantic Bight nitrogen budget. *Journal of Geophysical Research: Oceans*, *124*, 113–134. https://doi.org/10.1029/2018JC014424

Received 1 AUG 2018
Accepted 28 NOV 2018
Accepted article online 1 DEC 2018
Published online 4 JAN 2019

Abstract Understanding of nitrogen cycling on continental shelves, a critical component of global nutrient cycling, is hampered by limited observations compared to the strong variability on a wide range of time and space scales. Numerical models have the potential to partially alleviate this issue by filling spatiotemporal data gaps and hence resolving annual area-integrated nutrient fluxes. In this study, a three-dimensional biogeochemical-circulation model was implemented to simulate the Mid-Atlantic Bight (MAB) nitrogen budget. Model results demonstrate that, on average, MAB net community production (NCP) was positive (+0.27 Tg N/year), indicating net autotrophy. Interannual variability in NCP was strong, with annual values ranging between 0.19 and 0.41 Tg N/year. Along-shelf and across-shelf horizontal transport fluxes were the other dominant terms in the nitrogen budget and were primarily responsible for this NCP variability. The along-shelf current transported nitrogen from the north (0.65 Tg N/year) into the MAB, supplementing the nitrogen entering from terrestrial inputs (0.27 Tg N/year). However, NCP was highest in the year when total water volume transport and inorganic nitrogen input was strongest across the continental slope in the southern MAB, rather than when terrestrial inputs were greatest. Interannual variability of NCP appears to be linked to changes in the positions of the Gulf Stream and Slope Water Gyre. Overall, the strong spatiotemporal variability of the nitrogen fluxes highlights the importance of observations throughout all seasons and multiple years in order to accurately resolve the current status and future changes of the MAB nitrogen budget.

Plain Language Summary Portions of the ocean adjacent to land masses play a particularly important role in global nutrient cycling; however, strong spatial and temporal variability in these shallow regions of the ocean make it difficult to quantify nitrogen fluxes from observations alone. Here we use a computer simulation to estimate the fluxes and transformations of inorganic and organic nitrogen in Mid-Atlantic U.S. coastal waters. The coastal circulation flows southward providing roughly two thirds of the inorganic nitrogen to this region, with the remaining third entering from rivers and estuaries. Nitrogen transport across the continental slope is highly variable, directed into the system in some years and out in others. The net community production of the system, that is, the conversion of inorganic to organic nitrogen through photosynthesis minus respiration, is also highly variable. This strong interannual variability is primarily due to the highly variable fluxes of inorganic nitrogen entering this region from across the continental slope where the Gulf Stream approaches the continental slope, rather than the variability in terrestrial inputs. Overall, the strong variability of this region highlights the importance of collecting observations throughout all seasons and during multiple years in order to accurately resolve coastal nutrient budgets.

1. Introduction

Until recently, global biogeochemical cycling studies have underestimated the importance of continental shelves because these regions make up a relatively small proportion of total sea surface area (~8%). However, evidence is accumulating that continental margins may contribute significantly to global carbon

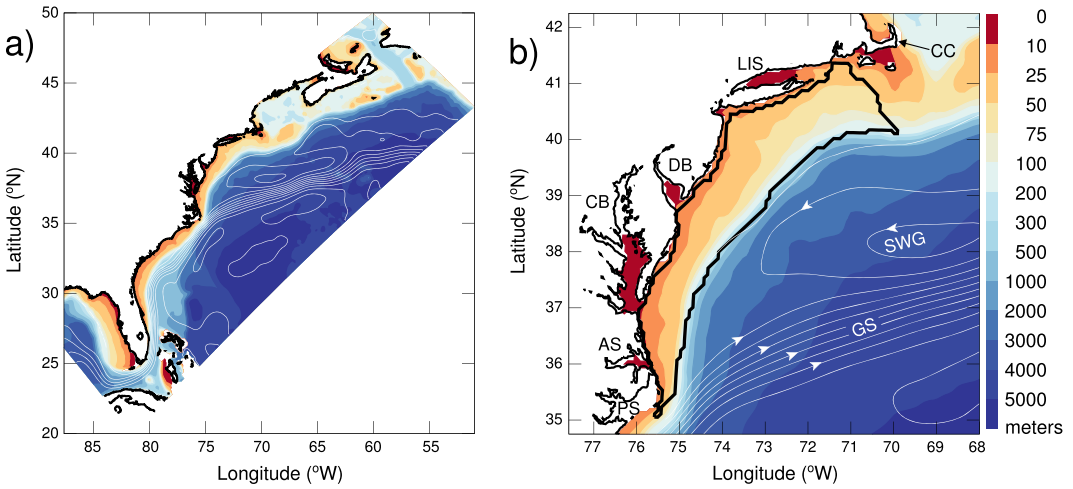

Figure 1. Maps of bathymetry for (a) full model domain and (b) inset of Mid-Atlantic region. White lines represent mean 10-cm contours of surface elevation where water depths exceed 200 m. In (b), the surface elevation lines highlight the location of the Gulf Stream (GS; parallel white lines) and the Slope Water Gyre (SWG; oval, north of the Gulf Stream). The black line in (b) represents the Mid-Atlantic Bight (MAB) study region. Locations shown include the following: Cape Cod (CC), Long Island Sound (LIS), Delaware Bay (DB), Chesapeake Bay (CB), Albemarle Sound (AS), and Pamlico Sound (PS).

and nitrogen cycles (C. T. A. Chen et al., 2003; Jahnke, 2010; Muller-Karger et al., 2005; Najjar et al., 2018). In spite of the relatively small area of continental shelves, observational studies often lack the space and time coverage that is needed to obtain annual estimates of continental shelf nitrogen fluxes. Coupled physical-biological numerical models can provide the space and time resolution that is needed to compute continental shelf nutrient fluxes and budgets (e.g., Cahill et al., 2016; Fennel et al., 2006, 2008; Hofmann et al., 2011, 2008; Kishi et al., 2007; Sasai et al., 2006; Schrum et al., 2006; St-Laurent et al., 2017; Wakelin et al., 2012; Xue et al., 2013). Such models are particularly useful for coastal systems where nutrient budgets are significantly impacted by anthropogenically changing terrestrial nutrient inputs and spatially and temporally varying circulation patterns.

The connection of coastal shelf waters to terrestrial and riverine inputs and oceanic waters provides an integration across systems that is critical in biogeochemical cycling and nutrient budgets. Increasing utilization of anthropogenic fertilizers and management actions in coastal watersheds have caused changes in riverine input of nitrogen to coastal waters over the last century (Galloway et al., 2004; Yang, Tian, Friedrichs, Hopkinson, et al., 2015). Modified ocean circulation due to mesoscale events (Mahadevan & Archer, 2000; McGillicuddy et al., 1998; Oschlies & Garcon, 1998; Siegel et al., 1999; S. Zhang et al., 2018) and/or climate change (Caesar et al., 2018; Ezer, 2015; Saba et al., 2016) also has the potential to impact nutrient inputs and cycling in coastal waters. Such changes in nitrogen inputs impact continental shelf net community production (NCP), defined here as the difference between the generation of organic nitrogen through photosynthesis and the conversion of organic nitrogen to inorganic nitrogen through respiration and remineralization processes. Nitrogen inputs to coastal systems can also be denitrified, buried, or advected to the open ocean. Quantifying each of these nitrogen fluxes, and their temporal and spatial variability, is critical to gaining a better understanding of both regional and global biogeochemical cycles.

The objective of this study is to quantify the spatiotemporal variability of key nitrogen fluxes in the Mid-Atlantic Bight (MAB) by implementing a three-dimensional coupled biogeochemical-circulation model. This region (Figure 1) is of particular interest because of the effect of interannual variability of physical processes (S. Zhang et al., 2018; W. G. Zhang & Gawarkiewicz, 2015), including climate-related changes in precipitation, temperature, and circulation (K. Chen et al., 2015; K. Chen & Kwon, 2018; Ji et al., 2007; Schulte et al., 2018) on biogeochemical cycling. This area is remotely affected by two large-scale currents (Linder & Gawarkiewicz, 1998; Linder et al., 2006): the northward flowing, warm, and low-nutrient Gulf Stream current and the southward flowing, cold, and nutrient-rich Labrador slope current, as well as the cyclonic Slope Water Gyre that occurs in between these two currents (Figure 1). This study builds on earlier efforts to better understand nitrogen fluxes in the MAB (e.g., Fennel, 2010) by forcing the coastal ocean model with inputs from

terrestrial (Tian et al., 2015; Yang, Tian, Friedrichs, Hopkinson, et al., 2015; Yang, Tian, Friedrichs, Liu, et al., 2015) and atmospheric nitrogen models (St-Laurent et al., 2017) and including dissolved organic nitrogen (DON) cycling as well as burial and resuspension (Druon et al., 2010).

This paper is structured as follows. Section 2 first describes the numerical models and nitrogen budget calculations, and then section 3 examines the results of a 5-year simulation of the MAB. These results describe the following: (1) the 5-year averaged nitrogen fluxes, (2) their seasonal variability, (3) their spatial variability, and (4) their interannual variability. Section 4 discusses these results in the context of past nitrogen flux studies of the MAB, examines the mechanisms causing the strong spatiotemporal variability of the NCP, and provides suggestions for future work. Lastly, the primary findings are briefly summarized in section 5.

2. Methods

2.1. Biogeochemical Ocean Circulation Model

The 3-D circulation model employed in this study is based on the Regional Ocean Modeling System (ROMS, Shchepetkin & McWilliams, 2005), a modeling system widely used for shelf circulation and coupled physical-biological applications (e.g., Cahill et al., 2016; Druon et al., 2010; Fennel et al., 2006; Hermann et al., 2009; He et al., 2011; Hofmann et al., 2011, 2008; St-Laurent et al., 2017; Xue et al., 2013; Wilkin, 2006). As in Hofmann et al. (2011), Cahill et al. (2016), and St-Laurent et al. (2017), ROMS is configured for the U.S. eastern continental shelf (Figure 1a) with a horizontal resolution of ~9 km and run for the mid-2000s (2004–2008 in this case). Bulk formulae (Fairall et al., 2003) are used to compute air-sea fluxes using air temperature, pressure, humidity, and winds from 3-hourly National Center for Environmental Prediction reanalysis fields (Mesinger et al., 2006). Physical and biological tracers are advected using the Multidimensional Positive Definite Advection Transport Algorithm (Smolarkiewicz & Margolin, 1998). Subgrid-scale vertical diffusivity is estimated using the parameterization from Mellor and Yamada (1982). All model formulations and parameters are identical to those described in St-Laurent et al. (2017) except for horizontal diffusion of temperature and salinity, which was increased slightly to improve simulations of the physical fields.

This circulation model is coupled to the USECoS (U.S. Eastern Continental Shelf) biogeochemical model that includes prognostic equations for two size classes of phytoplankton (P) and zooplankton (Z), semilabile and refractory DON, nitrate, ammonium, oxygen, and small and large carbon and nitrogen detrital pools. Although the model includes the full inorganic and organic carbon cycle as well (see St-Laurent et al., 2017, supporting information for detailed equations), it does not influence the nitrogen budget and thus is not discussed here. The degree of biogeochemical complexity (i.e., number of plankton size classes) chosen for this model was based on the model intercomparison results of Xiao and Friedrichs (2014a). By assimilating satellite-derived particulate organic carbon and size-fractionated chlorophyll concentrations, Xiao and Friedrichs (2014b) demonstrated that this "2P2Z" model had the highest level of model skill compared to simpler models with single phytoplankton and zooplankton size classes and compared to a more complex model with three phytoplankton state variables. Dissolved organic carbon (DOC) and DON represent key components of the nitrogen and carbon budget (Carlson et al., 2010; Fasham et al., 1999; Hansell & Carlson, 2001) yet are frequently not included in continental shelf nutrient cycle simulations (Fennel et al., 2006, 2008; He et al., 2011; Xue et al., 2013). As in Druon et al. (2010), DOC and DON are partially decoupled in order to allow for variations of C:N ratios due to preferential degradation of DON or C:N ratios of different sources (Hopkinson & Vallino, 2005). Full equations of the USECoS model are provided in the supporting information of St-Laurent et al. (2017).

An important nutrient source for the MAB is from the land, and this terrestrial linkage was included as part of the model setup through inputs from the 31 rivers included in the model domain. As in Feng et al. (2015) and St-Laurent et al. (2017), daily riverine freshwater and nutrient inputs are derived from the Dynamic Land Ecosystem Model (DLEM; Tian et al., 2010). DLEM is a process-based mechanistic terrestrial model, which provides explicit flux estimates of freshwater (Yang, Tian, Friedrichs, Liu, et al., 2015), carbon (Tian et al., 2015), and nitrogen (Yang, Tian, Friedrichs, Hopkinson, et al., 2015) from terrestrial ecosystems to river networks and eventually to the estuaries and coastal oceans of the U.S. eastern continental shelf. These fluxes are simulated through generation of surface runoff after precipitation events, leaching of these materials to river networks, transformation of carbon and nutrients in rivers and lakes, and transport from upstream areas to coastal regions. Extensive skill assessment with observations from the U.S. Geological Survey (Tian et al.,

2015; Yang, Tian, Friedrichs, Hopkinson, et al., 2015; Yang, Tian, Friedrichs, Liu, et al., 2015) shows that DLEM successfully captures seasonal and interannual variability in fluxes of freshwater, nitrogen, and carbon to the coastal zone of the eastern United States. In the Chesapeake Bay watershed, DLEM skill is similar to that of the Chesapeake Bay Watershed Model (Shenk & Linker, 2013) in terms of reproducing observed hydrological transports and loads of nitrate (Yang, Tian, Friedrichs, Hopkinson, et al., 2015; Yang, Tian, Friedrichs, Liu, et al., 2015).

Another important, yet often neglected, source of nitrogen to the coastal ocean is from atmospheric deposition. During the summer in the Gulf Stream region, atmospheric nitrogen deposition can increase surface nitrogen concentrations by 14% and increase new surface primary production by 22% (St-Laurent et al., 2017). In the Chesapeake Bay, atmospheric deposition has the same gram-for-gram impact on low oxygen concentrations (hypoxia) as riverine nitrogen loading (Da et al., 2018). Here atmospheric deposition estimates were obtained from the U.S. Environmental Protection Agency's Community Multiscale Air Quality (CMAQ) model (Appel et al., 2011; Gantt et al., 2015), as in St-Laurent et al. (2017), and are provided to the ocean model as 3-hourly fluxes of nitrate, ammonium, and DON to the ocean surface.

Boundary and initial conditions were similar to those used in St-Laurent et al. (2017). The open boundary conditions for the physical fields were obtained from 3-day averages of the Hybrid Coordinate Ocean Model North Atlantic assimilative model (Chassignet et al., 2007). The boundary conditions for nitrate and oxygen concentrations were derived from the World Ocean Atlas monthly climatology (Garcia et al., 2014a, 2014b), while boundary conditions for other biological variables were set to constant small values throughout the simulation period. These approximations do not deleteriously affect simulations within the MAB area since all boundaries were placed far from the study area. The initial conditions for the simulation were derived by repeatedly running the model over the period 2004–2008 (with the December 2008 state used to reinitialize the model on January 2004). As documented in St-Laurent et al. (2017), model skill has been extensively assessed based on nutrient concentrations from the World Ocean Atlas (Garcia et al., 2014a) and surface chlorophyll concentrations from the Sea-Viewing Wide Field-of-View Sensor (National Aeronautics and Space Administration, 2014).

2.2. Nitrogen Budget Calculations

The USECoS model is used to compute the total nitrogen (TN) budget in the MAB over the full water column. For the purposes of these budget calculations, the MAB is defined as the region along the continental shelf extending roughly from the 10- to 15-m isobath to the 200-m isobath (Figure 1b). The TN budget is expressed as the time rate of change of TN ($\partial(\mathrm{TN})/\partial t$) balancing the sources and sinks of nitrogen due to atmospheric deposition ($\mathrm{AtmDep_{TN}}$), denitrification ($\mathrm{Denit_{TN}}$), burial ($\mathrm{Burial_{TN}}$), and horizontal transport:

$$\partial(\mathrm{TN})/\partial t = \mathrm{AtmDep_{TN}} + \mathrm{Denit_{TN}} + \mathrm{Burial_{TN}} + \mathrm{E\&R_{TN}} + \mathrm{Ocean_{TN}} \quad (1)$$

where horizontal transport is separated into the component entering from the land side of the model domain (estuaries and rivers = $\mathrm{E\&R_{TN}}$) and the oceanic side of the model domain ($\mathrm{Ocean_{TN}}$). Horizontal transport on the oceanic side of the model domain can be further subdivided into the flux along the shelf from the north (northeast; $\mathrm{NE_{TN}}$) and that crossing the offshore MAB boundary (continental slope; $\mathrm{CS_{TN}}$). The horizontal transport terms include advection and turbulent diffusion, but the latter is generally insignificant. Equation (1) has dimensions of mass per unit time, with a positive flux indicating nitrogen accumulation within the MAB and a negative flux indicating nitrogen loss. Thus, denitrification and burial are always negative, and atmospheric deposition is always positive. The horizontal transport terms can be either positive or negative.

The budget for dissolved inorganic nitrogen (DIN) and total organic nitrogen (TON) are similarly computed as follows:

$$\partial(\mathrm{DIN})/\partial t = \mathrm{AtmDep_{DIN}} + \mathrm{Denit_{DIN}} + \mathrm{E\&R_{DIN}} + \mathrm{Ocean_{DIN}} - \mathrm{NCP} \quad (2)$$

$$\partial(\mathrm{TON})/\partial t = \mathrm{AtmDep_{TON}} + \mathrm{Burial_{TON}} + \mathrm{E\&R_{TON}} + \mathrm{Ocean_{TON}} + \mathrm{NCP} \quad (3)$$

where NCP transforms inorganic nitrogen to organic nitrogen and thus appears as equal and opposite terms in the above two equations. Although N_2 fixation may be an important source term for DIN at certain times of

year in this region (Mulholland et al., 2012), on annual scales it represents a small (<5%) change in DIN compared to that due to productivity. As a result, it is not included in the USECoS model and hence is not a component of the budget presented here. Within the USECoS model, all the nitrogen associated with the phytoplankton, zooplankton, and detritus state variables are considered particulate organic nitrogen (PON), and DIN represents the only inorganic nitrogen pool. In contrast, TON has two components: PON and DON.

3. Results

3.1. Model Estimates of the 5-Year Mean Nitrogen Budget

The distributions of the various forms of nitrogen within the MAB provide insights into variability of the nitrogen fluxes. Surface concentrations of DIN (defined as the sum of the modeled nitrate and ammonium state variables), DON (defined as the sum of the semilabile DON and refractory DON state variables) and PON (defined as the sum of the phytoplankton, zooplankton, and detrital state variables) were higher within the MAB than in waters located off the continental shelf (Figures 2a, 2c, and 2e). Concentrations were particularly high where estuaries and rivers flowed to the shelf, such as in the vicinity of the Chesapeake Bay, Delaware Bay, and Long Island Sound plumes. Concentrations of DON were high throughout most of the MAB (Figure 2c), whereas high concentrations of DIN were restricted closer to the shore (Figure 2a). Throughout much of the MAB, surface concentrations of PON were approximately half that of DON (Figures 2c and 2e). At 100-m depth, concentrations of DIN (Figure 2b) were high in the region north of the Gulf Stream and in the Slope Water Gyre south of Cape Cod (Figure 1b), due to shoaling isopycnals north of the Gulf Stream that upwell deep nitrate-rich waters (Csanady & Hamilton, 1988). In contrast, DON and PON concentrations were relatively low at 100 m (Figures 2d and 2f). Neither DON nor PON concentrations show a gradient across the Gulf Stream at depth (Figures 2d and 2f), whereas DIN concentrations throughout the water column show a strong gradient across the Gulf Stream with higher concentrations to the north than to the south, (Figures 2a and 2b).

Temporal averaging of equation (2) provides an estimate for the 2004–2008 mean inorganic nitrogen budget (Figure 3). Over this 5-year period, DIN sources (0.39 Tg N/year) essentially balance DIN sinks (0.37 Tg N/year). Most of the DIN source (85%) is from horizontal transport ($E\&R_{DIN} + NE_{DIN}$) with the northeast transport dominating, and the remaining 15% coming from atmospheric deposition. NCP is positive, indicating overall net autotrophy of the MAB, and accounts for 73% of the DIN sink, with the remaining losses split roughly equally between denitrification and horizontal transport across the shelf break (CS_{DIN}). Hence, the first-order DIN balance is one of horizontal transport inputs balancing NCP.

Horizontal transport and NCP also play dominant roles in the 2004–2008 mean organic nitrogen budget (Figure 3). Of the TON sources, which total 0.87 Tg N/year and balance the TON sinks, horizontal transport from the northeast (NE_{TON}) and NCP account for 51% and 31%, respectively. Horizontal transport from estuaries and rivers ($E\&R_{TON}$) accounts for most of the remaining 18%, with a very small role played by atmospheric deposition (St-Laurent et al., 2017). Nearly all (95%) of the TON sink is due to cross-shelf transport with burial accounting for the remaining 5%. Even though PON concentrations are much lower than DON concentrations at the northeast and continental shelf boundaries (Figure 2), PON and DON contribute roughly equally to transport across these boundaries.

Quantifying the water budget of the MAB is helpful for interpreting the nitrogen budget (Table 1). On average over the 5 years analyzed, water enters the MAB via estuaries and rivers (~7%) and from the northeastern along-shelf current (~93%) and flows out across the continental slope (Table 1). Although precipitation, evaporation, and changes in the average volume of water within the MAB cause small residuals between the horizontal transport sources and sinks on an annual basis (generally <2 mSv), over the 5-year simulation the amount of water entering from the landward side of the MAB ($E\&R = +6 \pm 1$ mSv) roughly balances the sum of the fluxes across the northeast and continental slope boundaries ($NE + CS = -7 \pm 2$ mSv; Table 3). This is because the CS and NE fluxes are typically large and have opposite sign in each of the 5 years analyzed. On average, the flux across the continental slope ($CS = -87 \pm 60$ mSv) is 7 mSv larger than that entering from the northeast ($NE = 80 \pm 59$ mSv). The large standard deviations on these estimates represent the significant interannual variability (see section 3.4) resulting from episodic events such as warm core rings interacting with the continental shelf (K. Chen et al., 2014). This general circulation pattern follows the concept of a

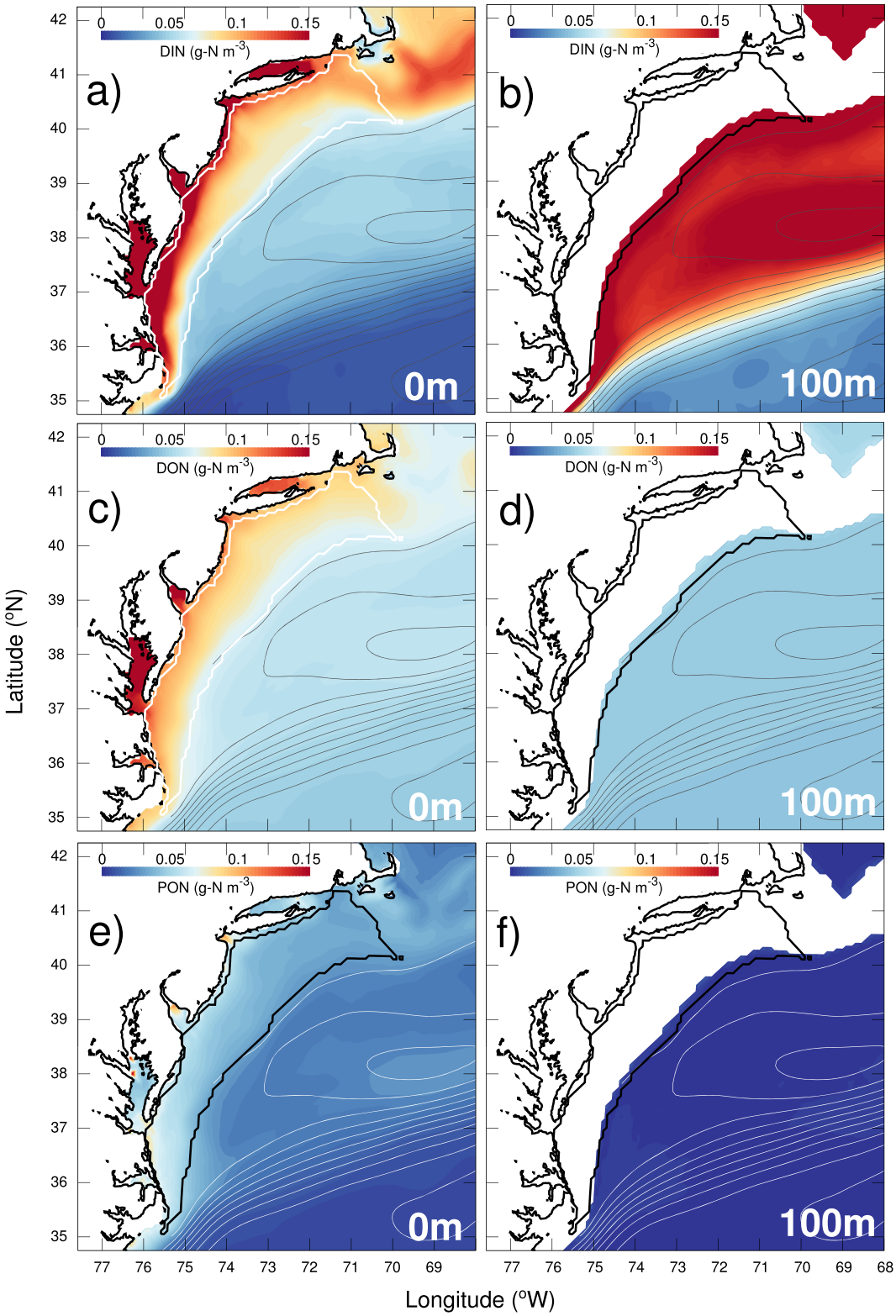

Figure 2. Average (2004–2008) concentrations of (a, b) dissolved inorganic nitrogen (DIN), (c, d) dissolved organic nitrogen (DON), and (e, f) particulate organic nitrogen (PON) at the surface (a, c, and e) and at 100 m (b, d, and f). Thick lines represent the Mid-Atlantic Bight study region. Thin lines represent mean 10-cm contours of surface elevation where water depths exceed 200 m.

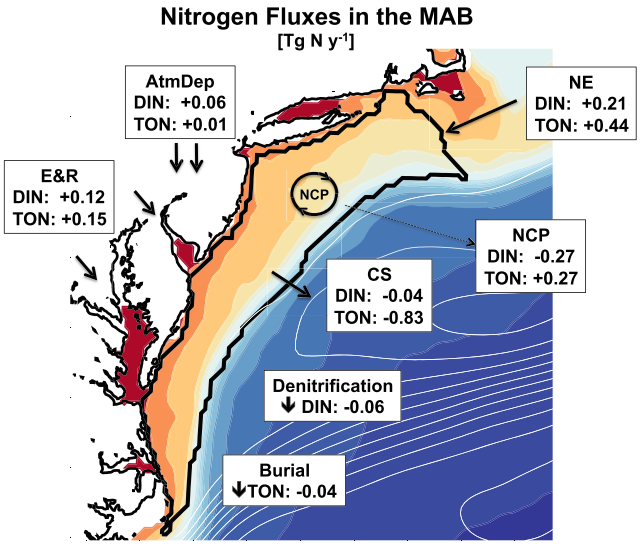

Figure 3. Five-year mean nitrogen budget (2004–2008) for the MAB study region, shown on top of the bathymetry and mean sea surface height of Figure 1b. All values are in teragrams of nitrogen per year. Positive numbers are sources to the MAB, and negative numbers are sinks.
AtmDep = atmospheric deposition; NCP = net community production; E&R = fluxes from the estuaries and rivers; CS = flux across continental slope; and NE = flux from the northeast. Standard deviations of 5-year means are provided in Tables 1 and 2; water transports are provided in Table 3.
MAB = Mid-Atlantic Bight; DIN = dissolved inorganic nitrogen; TON = total organic nitrogen.

"leaking" MAB shelf (Lozier & Gawarkiewicz, 2001) characterized by a decrease in along-shelf flow from the northeastern boundary of the MAB to Cape Hatteras (Levin et al., 2018). The strong interannual variability of both the along-shelf and the cross-shelf transports is also consistent with those determined from previous studies (e.g., K. Chen & He, 2015).

3.2. Seasonal Variability of Nitrogen Fluxes

The nitrogen budget terms showed varying levels of seasonal variability throughout the year (Figure 4). Atmospheric deposition was the least seasonally variable, with fluxes varying by only about 0.02 Tg N/year. Burial and denitrification both demonstrated a larger seasonal cycle, with highest fluxes in the spring when primary production is high and lowest fluxes in winter (Figures 4a, 4c, and 4e). As described above, nitrogen input from the land was the smallest of the three horizontal transport fluxes (Figure 3); however, some seasonal variability is still apparent (Figures 4b, 4d, and 4f). Organic nitrogen input from the estuaries and rivers to the MAB is greatest in the summer, which is when the greatest productivity of organic matter within the coastal estuaries typically occurs (Harding et al., 2002). In contrast, input of DIN to the MAB from the estuaries and rivers is typically least in summer, since during this time of year (1) DIN is being rapidly taken up inside the estuaries and (2) river runoff is typically low.

Seasonal variability was particularly prominent in the along-shelf and across-shelf physical horizontal fluxes (Figures 4b, 4d, and 4f). Specifically, horizontal fluxes of both organic and inorganic nitrogen from the NE were highest in spring, which is also when the along-shelf water transport is greatest (Figure 4g). From September to December, the fluxes across the northeastern MAB boundary were smallest and even reversed direction (flowing out of the MAB) during some of this time, again consistent with the water transports across this boundary (Figure 4g). It is important to note, however, that this seasonal variability in along-shelf and across-shelf transport varies considerably from year to year, making it difficult to assess the skill of model results with observations such as those of Lentz (2008a, 2008b). The seasonality in TN flux across the continental slope roughly mirrored that across the northeastern MAB boundary (Figure 4b). Organic nitrogen was directed across the shelf and out of the MAB all year long with the highest flux being in spring (Figure 4f). The flux of inorganic nitrogen across the continental slope was highly variable throughout the year (Figure 4d) and did not always follow the organic nitrogen or water transport fluxes (Figure 4g). This overall seasonal variability can be put into perspective by comparing the results shown in Figure 4 to the interannual variability (standard deviations) presented in Tables 1–3.

The NCP flux showed the largest seasonal amplitude. This term, representing the conversion of inorganic nitrogen to organic nitrogen (Figures 4d and 4f), was greatest during the spring bloom period and least in the time period directly following the spring bloom, which is a time of rapid recycling. A smaller positive peak of NCP occurred in fall (September) and was again followed by a period of net heterotrophy (negative NCP) from October to December (Figure 4f). The seasonal variability of NCP was largely responsible for the seasonality of the rate of change terms, particularly for organic nitrogen, that is, NCP $\approx \partial \mathrm{TON}/\partial t$ (Figure 4f).

Table 1
Magnitude of Horizontal Water Flux Terms (mSv = 10^3 m^3/s)

Year	Estuaries & rivers (E&R)	Northeast (NE)	Continental slope (CS)	Ocean flux (NE + CS)
2004	+7	+93	−100	−7
2005	+6	+154	−160	−6
2006	+7	+64	−73	−9
2007	+5	−7	+4	−3
2008	+6	+97	−105	−8
2004–2008 Mean	+6	+80	−87	−7
± Std. Dev.	±1	±59	±60	±2

3.3. Spatial Variability of Nitrogen Fluxes

Atmospheric deposition, NCP, burial, and denitrification varied spatially throughout the study region (Figure 5). Of these flux terms, atmospheric deposition was the least spatially variable within the MAB (Figure 5a), though farther offshore a high band of atmospheric deposition occurs over the Gulf Stream due to very high precipitation in that region (St-Laurent et al., 2017). In contrast, NCP was highly variable within the MAB, with the highest values occurring in the south and along the continental

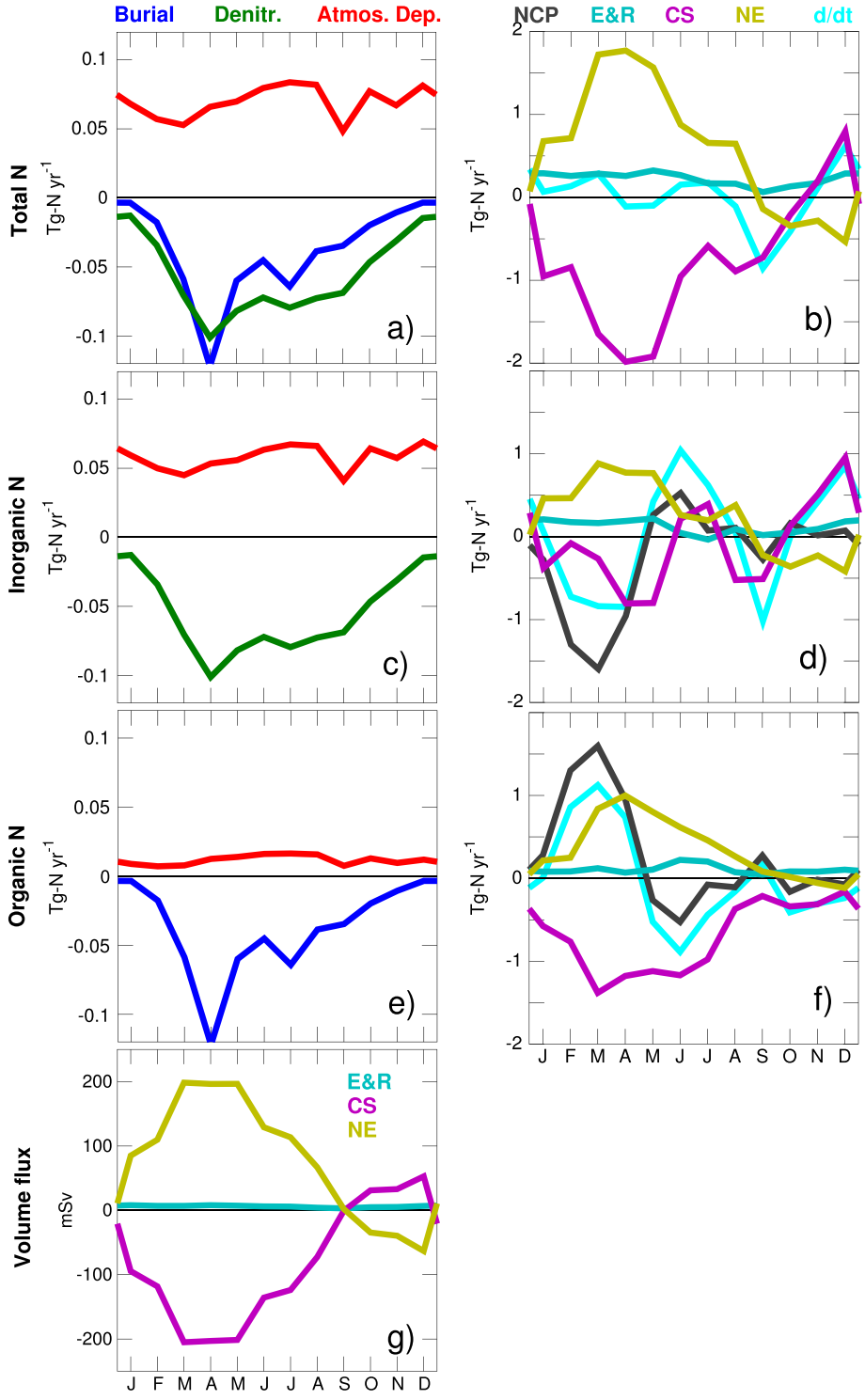

Figure 4. Monthly variability of 5-year mean (2004–2008) budget terms shown in Figure 3, for (a, b) total nitrogen, (c, d) dissolved inorganic nitrogen, and (e, f) total organic nitrogen. (a), (c), and (d) show atmospheric deposition, denitrification, and burial. (b), (d), and (f) show net community production (NCP), as well as horizontal fluxes from the estuaries and rivers (E&R), across the continental slope (CS), and from the northeast (NE) as defined in Figure 3. Note the change in scale in (b), (d), and (f) compared to (a), (c), and (e). Water volume transport fluxes are shown in (g).

Table 2
Magnitude of Nitrogen Budget Terms (Tg N/Year)

	Horizontal flux[a]			Atmospheric deposition		Burial	Denitrification	NCP	∂/∂t
Year	DIN	DON	PON	DIN	DON	PON	DIN	TON	TN
2004	+0.01	−0.10	−0.12	+0.06	+0.01	−0.04	−0.06	+0.26	−0.24
2005	+0.28	−0.09	−0.08	+0.05	+0.01	−0.03	−0.05	+0.21	+0.07
2006	+0.26	−0.08	−0.09	+0.07	+0.01	−0.04	−0.06	+0.19	+0.07
2007	+0.38	−0.19	−0.20	+0.06	+0.01	−0.04	−0.06	+0.41	−0.05
2008	+0.49	−0.12	−0.15	+0.06	+0.01	−0.05	−0.06	+0.29	+0.18
2004–2008 Mean	+0.28	−0.12	−0.13	+0.06	+0.01	−0.04	−0.06	+0.27	+0.006
± Std. Dev.	±0.18	±0.04	±0.05	± 0.01	±0.001	±0.01	±0.007	±0.09	±0.16

Note. The area of the MAB as defined here is 8.5714×10^4 km^2. DIN = dissolved inorganic nitrogen; DON = dissolved organic nitrogen; PON = particulate organic nitrogen; NCP = net community production, TON = total organic nitrogen..
[a]Horizontal flux includes all three terms listed in Table 3.

slope and lower values occurring in the midshelf portion of the MAB (Figure 2b). High NCP also occurred northeast of the MAB near Cape Cod (Figure 1b), while a region of low NCP occurred just southwest of this region in the northernmost portion of the MAB. Like NCP, the spatial variability of burial and denitrification within the MAB (Figures 5c and 5d) was also much larger than that of atmospheric deposition. The largest fluxes generally occurred in the shallowest waters closest to shore. Regions of higher burial and denitrification generally occurred where resuspension was low and/or where NCP was high (Figure 5b).

The 5-year mean horizontal transport fluxes of DIN (Figure 6a) and TON (Figure 7a) into and out of the MAB were also characterized by strong spatial variability. The flux of nitrogen from the estuaries and rivers was, as expected, largest near the outflow of major coastal water bodies, such as Pamlico Sound, Chesapeake Bay, Delaware Bay, and Long Island Sound (Figure 1b) and small in between (Figures 6a and 7a). The nitrogen entering the MAB from the northeast occurred over a much shorter along-boundary distance and showed less spatial variability across this boundary. Along the continental slope (CS), DIN entered from the south near the confluence of the Gulf Stream and the Slope Water Gyre (36.5°N, 74.5°W; Figure 6a) and exited the MAB along the continental slope north of the Slope Water Gyre. Horizontal transport fluxes of TON were directed out of the MAB across almost the entire continental slope (Figure 7a). The one exception was the small flux of organic matter into the MAB in the southern portion of the domain where the Gulf Stream comes closest to the outer shelf before turning out to the open ocean. In general, the transport of nitrogen into the MAB from the rivers and from the northeast and out of the MAB across the continental shelf was dictated by the total volume water transport of the system (Figure 8a).

3.4. Interannual Variability of Nitrogen Fluxes

Some of the terms in the nitrogen budget demonstrated strong interannual variability, while other terms showed much less interannual variability (Figure 9). The differences between the maximum and minimum annual burial, denitrification, and atmospheric nitrogen deposition fluxes were all very small (~0.02 Tg N/year;

Table 3
Magnitude of Horizontal Flux Terms (Tg N/Year)

	Estuaries and rivers (E&R)			Northeast (NE)			Continental slope (CS)		
Year	DIN	DON	PON	DIN	DON	PON	DIN	DON	PON
2004	+0.15	+0.05	+0.07	+0.40	+0.22	+0.15	−0.54	−0.37	−0.34
2005	+0.13	+0.05	+0.08	+0.30	+0.39	+0.29	−0.15	−0.53	−0.45
2006	+0.12	+0.05	+0.12	+0.16	+0.20	+0.22	−0.02	−0.33	−0.43
2007	+0.08	+0.05	+0.09	−0.16	+0.05	+0.09	+0.46	−0.29	−0.38
2008	+0.10	+0.05	+0.12	+0.33	+0.30	+0.28	+0.06	−0.47	−0.55
2004–2008 Mean	+0.12	+0.05	+0.10	+0.21	+0.23	+0.21	−0.04	−0.40	−0.43
± Std. Dev.	±0.03	±0.00	±0.02	±0.22	±0.13	±0.09	±0.36	±0.10	±0.08

Note. DIN = dissolved inorganic nitrogen; DON = dissolved organic nitrogen; PON = particulate organic nitrogen.

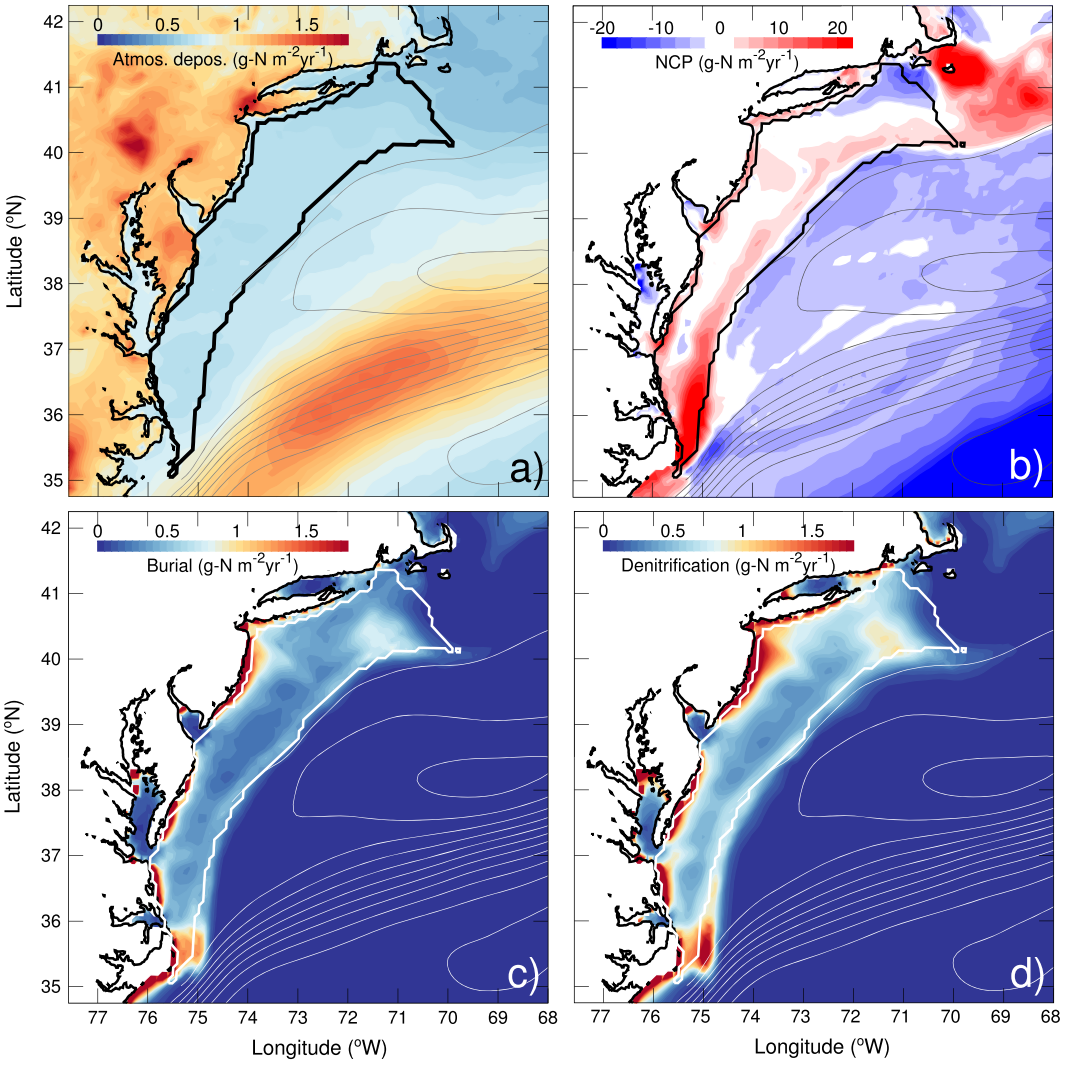

Figure 5. Spatial distribution of mean budget terms shown in Figure 3: (a) atmospheric nitrogen deposition (dissolved inorganic nitrogen + dissolved organic nitrogen), (b) net community production (NCP), (c) burial, and (d) denitrification. Note that (b) is shown on a different scale than the other three panels.

Table 2). In comparison, the flux of nitrogen from the estuaries and rivers was more variable, with the lowest flux occurring in 2007 ($E\&R_{TN}$ = 0.22 Tg N/year), and the highest occurring in 2006 ($E\&R_{TN}$ = 0.29 Tg N/year; Figure 9 and Table 3), and with the variability being much greater for PON and DIN than for DON (Table 3). Although the total E&R flux varied from year to year, the locations of greatest flux stayed relatively constant (Figures 6 and 7). Specifically, the locations of greatest export in each year continued to be in the vicinity of the outflow of major coastal water bodies, such as Pamlico Sound, Chesapeake Bay, Delaware Bay, and Long Island Sound.

The horizontal advective flux from the northeast and across the continental slope was considerably more variable than the flux from estuaries and rivers. This large variability in the NE_{TN} + CS_{TN} flux (−0.22 ± 0.16 Tg N/year) was primarily driven by the highly variable DIN flux across the continental slope, (CS_{DIN} = −0.04 ± 0.36 Tg N/year), which overall was directed seaward in some years (2004–2006) and landward in others (2007 and 2008; Table 3 and Figure 6). Specifically, as the convergence region between the Gulf Stream and Slope Water Gyre migrated north and south from one year to another, the location of maximum flux of DIN into the MAB along the continental slope also shifted north and south (Figures 6b–6f). This location was farthest north in 2007 due to the presence of a Gulf Stream meander in the region (Figure 6e), which was also the year with the greatest total flux of DIN into the MAB along the continental slope (Table 3).

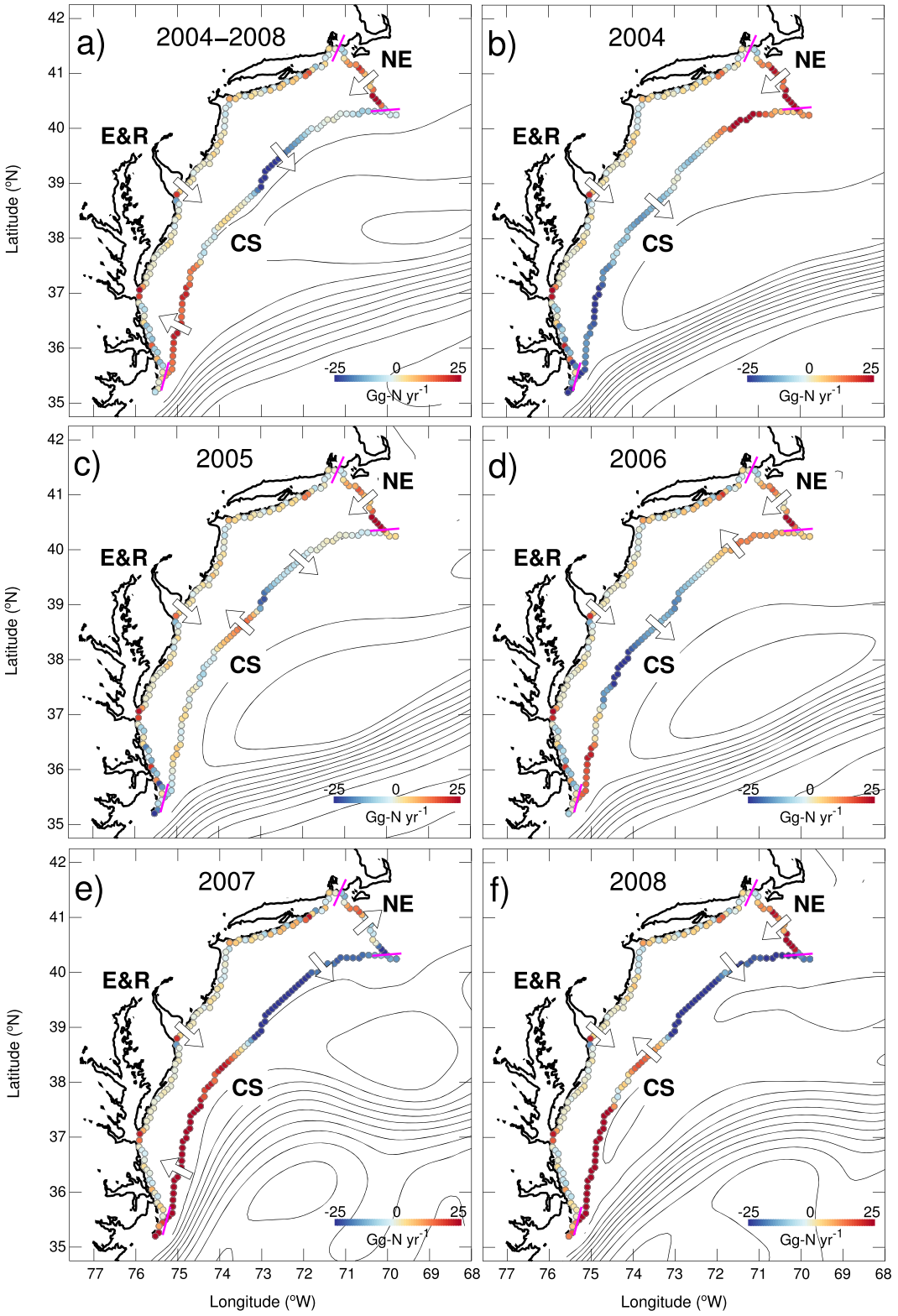

Figure 6. Spatial distribution of annual dissolved inorganic nitrogen physical horizontal fluxes for (a) 2004–2008, (b) 2004, (c) 2005, (d) 2006, (e) 2007, and (f) 2008, including fluxes from the estuaries and rivers (E&R), the northeast (NE), and across the continental slope (CS). Flux across each model grid cell is shown with a smoothing along the boundary for clarity. Pink lines denote separations between these three regions.

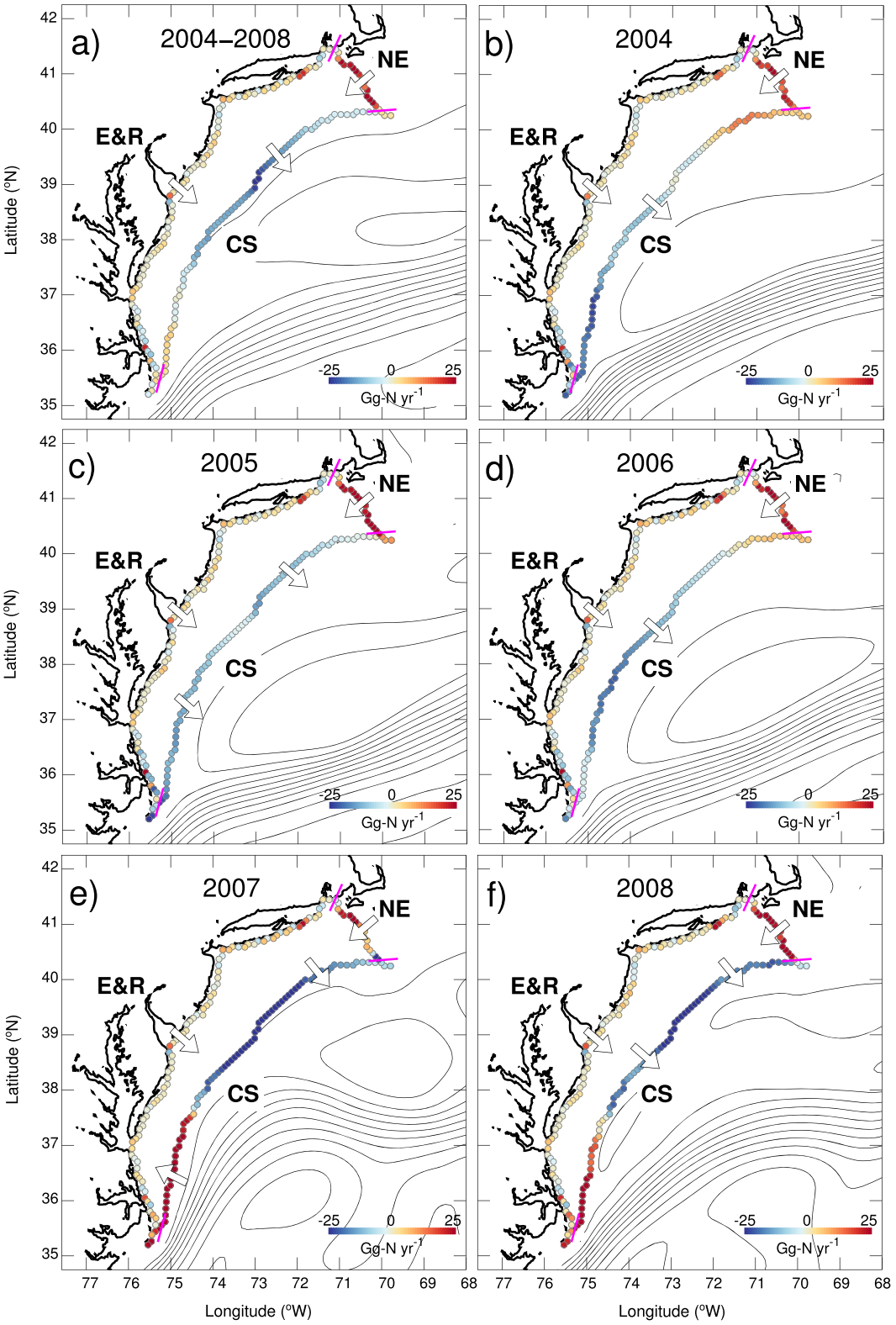

Figure 7. As in Figure 6 but for total organic nitrogen.

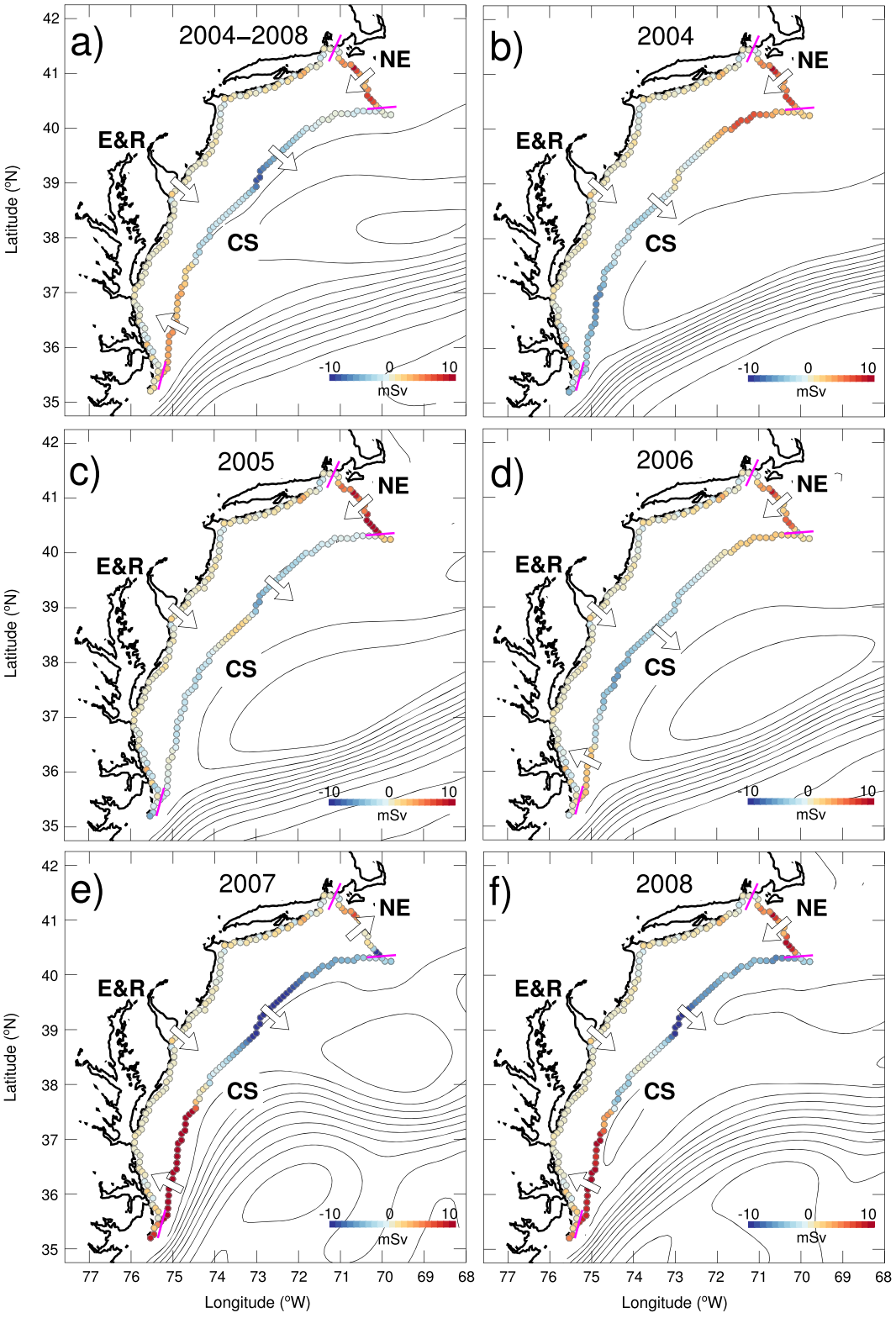

Figure 8. As in Figure 6 but for total water volume transport (1 mSv = 10^3 m^3/s.)

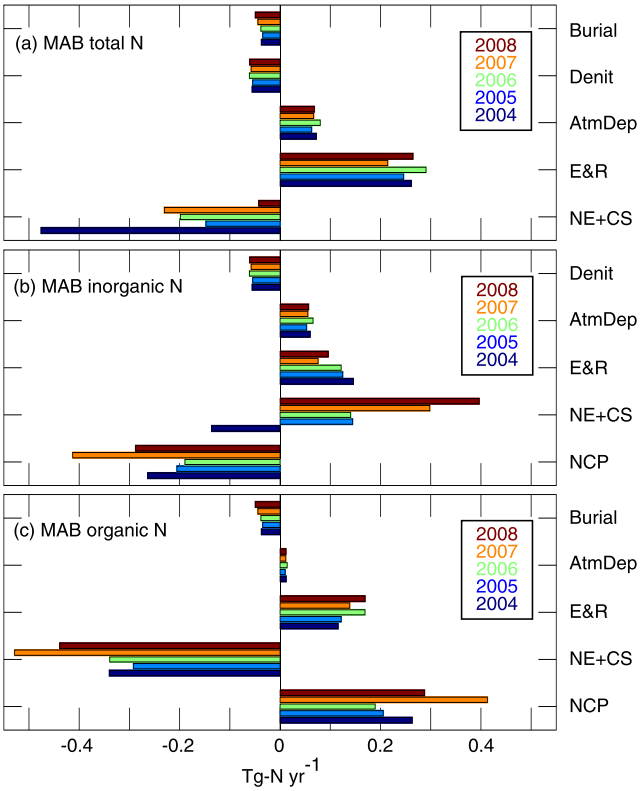

Figure 9. Interannual variability of mean (2004–2008) budget terms shown in Figure 3. (Note that the CS and NE fluxes are combined, since their magnitudes are large and often opposite.) CS = continental slope; NE = northeast; MAB = Mid-Atlantic Bight; NCP = net community production; E&R = estuaries and rivers; AtmDep = atmospheric deposition.

Although the flux of DIN across the northeastern boundary of the MAB was generally directed into the MAB, 2007 was an anomalous year in that the net flux of DIN across this boundary was directed out of the MAB. In terms of water flux (Table 1 and Figure 8), 2007 was also an anomalous year, in that it was the only year in which the net water transport was directed out of the MAB along the northeastern boundary from the northeast and into the MAB across the continental slope. Although the individual CS and NE fluxes were anomalous in 2007 for both DIN and water transport, the overall flux was very similar in 2007 (CS_{TN} + NE_{TN} = −0.23 Tg N/year) to the 5-year mean (CS_{TN} + NE_{TN} = −0.22 Tg N/year; Table 3).

NCP also varied considerably throughout the 5 years (NCP = 0.27 ± 0.09 Tg N/year; Figure 8 and Table 2). The annual mean NCP was highest in 2007 (>0.4 Tg N/year). Interestingly, this was the year of lowest terrestrial input to the MAB but greatest input of DIN across the continental slope (Table 3). The net horizontal flux of organic nitrogen out of the MAB was also largest in 2007 (Table 2). Analogously, the mean annual NCP was lowest in 2005 and 2006, which was also the year of lowest horizontal flux of organic nitrogen out of the MAB (−0.17 Tg N/year in both years.)

4. Discussion

4.1. Comparison of Modeled Nitrogen Budget to Prior Estimates

The modeled nitrogen flux terms computed for the 5-year mean (Figure 3) are generally consistent with previous observations and model simulations, given the 5-year standard deviations of the model estimates (Tables 2 and 3). This agreement is particularly noteworthy since (1) in highly variable areas like the MAB observations with sufficient spatial and temporal coverage to estimate annual flux estimates for the full region are lacking and (2) models are inherently associated with significant errors due to uncertain parameterizations. The simulated burial rates estimated over the full MAB area (8.5714×10^4 km^2) yield an annual mean areal burial rate of 0.47 g $N{\cdot}m^{-2}{\cdot}year^{-1}$. Assuming a Redfield C:N ratio, this rate is highly consistent with the carbon burial rate reported in Najjar et al. (2018) for the MAB (2.8 g $C{\cdot}m^{-2}{\cdot}year^{-1}$ = 0.49 g $N{\cdot}m^{-2}{\cdot}year^{-1}$). Denitrification rates vary substantially throughout the MAB (Figure 5d; Laursen & Seitzinger, 2002; Seitzinger & Giblin, 1996). The rate estimated in this study (~0.1 Tg N/year) was lower than the model results of Fennel (2010) for 2004–2005 (~0.4 Tg N/year), a difference that may result from the more sophisticated sediment boundary conditions applied in this study that account for resuspension and burial (Druon et al., 2010). Also, Fennel (2010) did not include DON or a second smaller class of phytoplankton as part of the model structure.

Horizontal transport fluxes across the MAB boundaries are difficult to estimate from observations alone due to their strong spatiotemporal variability and are thus most frequently estimated by modeling studies or mass balance approaches. For example, using an estuarine mass balance approach, Herrmann et al. (2015) estimated that 1.1–1.3 Tg C/year of organic carbon entered the MAB from estuaries. When converted with a Redfield ratio, this yields 0.19–0.23 Tg N/year, corresponding reasonably well with the estimate obtained here (0.15 ± 0.05 Tg N/year; Figure 3). Using a combined remote sensing and neural network approach for the years 2010–2012, Mannino et al. (2016) estimated the DOC flux from estuaries and rivers to the MAB as 0.8 Tg C/year. Assuming a C:N ratio for DOC of 15 mole C: mole N (Hopkinson & Vallino, 2005; Mannino et al., 2016), this yields a DON flux of 0.06 Tg N/year, which is similar to the estimate computed here of 0.05 Tg N/year (Table 3). Mannino et al. (2016) also computed a net outward horizontal flux of DOC of 2.6 Tg C/year for the MAB. Again converting this to DON using the C:N ratio of 15 mole C: mole N yields a net flux out of the MAB of −0.20 Tg N/year. This is only slightly larger than the 5-year mean (2004–2008) computed here by summing the transport in from the northeast, estuaries and rivers, and out across the continental slope (−0.12 ± 0.04 Tg N/year; Table 2). Considering the strong interannual variability of these flux estimates,

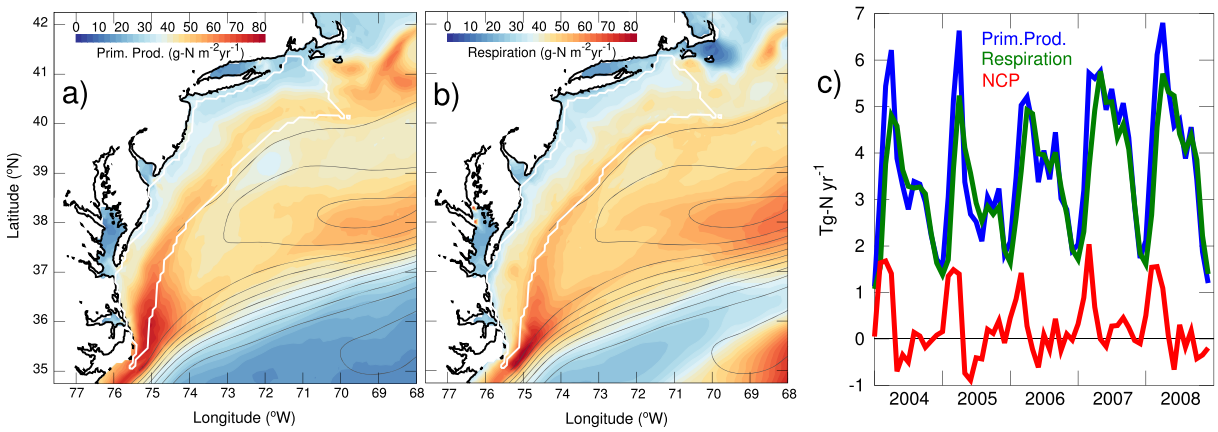

Figure 10. Five-year averaged nitrogen (a) primary production and (b) respiration; white line shows the outline of the Mid-Atlantic Bight region. (c) Time series of monthly averaged primary production, respiration, and net community production (NCP).

which range from a minimum in 2006 (−0.08 Tg N/year) to a maximum in 2007 (−0.19 Tg N/year; Table 2), and the very different approaches taken in deriving these estimates, the agreement between them provides increased confidence in these results.

The horizontal transport fluxes derived here are also similar to those of Fennel (2010), which used a similar physical model but a simpler biogeochemical model (no burial or resuspension, no dissolved organic matter, and only one phytoplankton size class) and used U.S. Geological Survey information directly without linking to a sophisticated terrestrial ecosystem model. Despite these differences, their estimate of TN entering from the estuaries and rivers (+0.22 Tg N/year) is consistent with that estimated here (+0.27 Tg N/year), especially given that their estimate did not include input of DON (~0.05 Tg N/year; Table 3). The modeled estimates for horizontal transport fluxes into and out of the MAB (Figure 3 and Table 2) also compare reasonably well to those in Fennel (2010). The net horizontal fluxes of DIN and PON calculated by Fennel (2010), 0.41 and −0.07 Tg N/year, respectively, were similar to those found in this study (0.28 ± 0.18 and −0.13 ± 0.05 Tg N/year; Table 2), especially considering that different years were analyzed in the analyses. The similarity suggests that, in spite of large interannual variability and differences in model structure, the basic processes controlling these fluxes are well represented in these models.

Long-term averaged estimates of net ecosystem production are almost nonexistent for the MAB; however, the modeled annual total production of organic nitrogen (and carbon) through photosynthesis (Figure 10a) was found to show a reasonable agreement to values in the literature. The modeled estimates of primary production obtained from this study (3.7 ± 0.5 Tg N/year; 22 ± 3 Tg C/year) were lower than historical estimates (30 Tg C/year) based on National Marine Fisheries Surveys conducted in the late 1970s and early 1980s (Najjar et al., 2018; O'Reilly et al., 1987). However, the estimate derived here is similar to estimates based on satellite productivity algorithms for the specific years analyzed here (K. Hyde, personal communication July 23, 2018; 24 Tg C/year). In addition, the model estimated areal primary production rate at the inner shelf (21 mol C·m^{-2}·year^{-1}) was within the range of primary production rates (6–45 mol C·m^{-2}·year^{-1}) observed in the southern MAB (Filippino et al., 2011).

4.2. Spatiotemporal Variability of NCP

This study is a first attempt to quantify the spatiotemporal variability of NCP, which is a critical term in the nitrogen budget. The model simulations show that NCP is highly variable over the MAB shelf, with the greatest rates occurring in the south (Figure 5b), where the Gulf Stream approaches the MAB boundary and intrusions of deep high nutrient water (S. Zhang et al., 2018) stimulate high productivity (Figure 10a). In general, NCP was higher along the continental slope than in the midshelf portion of the MAB (Figure 2b), again due to higher productivity stimulated by deep nutrient entrainment into the MAB euphotic zone via isopycnal shoaling along the shelf break (Ryan et al., 1999; Schollaert et al., 2004; S. Zhang et al., 2018). The resulting enhanced biological productivity at the shelf break is thus a subsurface feature and not evident from

satellite-derived surface productivity estimates (Kuring et al., 1990), which tend to decrease monotonically away from the coast.

The simulated spatial distributions of productivity and respiration (Figures 10a and 10b) each show similar patterns, but with opposite signs. This indicates that for the most part, organic nitrogen generated through primary production is respired locally. Exceptions exist, such as the region of high NCP associated with the relatively shallow topography south of Cape Cod (Figures 1b and 5b), an area known for strong upwelling and high productivity (Blanton et al., 1981; W. G. Zhang & Gawarkiewicz, 2015). The simulated patterns show this is a region of high productivity (Figure 10a) but low respiration (Figure 10b), leading to particularly high NCP (Figure 5b). In this case organic matter produced in this region is advected downstream (southwestward) where it is remineralized in the northern coastal MAB in a region of net heterotrophy, that is, where respiration exceeds primary production (Figures 10a and 10b).

Seasonal variability of NCP is large (Figures 4d and 4f) and is matched in magnitude only by the time rate of change terms ($\partial/\partial t$) as inorganic nitrogen is converted to organic nitrogen through primary production in the spring ($\partial \mathrm{DIN}/\partial t < 0$ and $\partial \mathrm{TON}/\partial t > 0$) and organic nitrogen is then converted back into inorganic nitrogen through respiration and remineralization processes in the early summer ($\partial \mathrm{TON}/\partial t < 0$ and $\partial \mathrm{DIN}/\partial t > 0$). Thus, NCP is greatest in the spring and typically becomes negative in the early summer, as recycling begins to dominate (Figure 4d). This pattern reflects the interaction between primary production and respiration (Figure 10c), with both following the same pattern of being largest in the spring and smallest in winter (Xu et al., 2013). However, spring primary production is slightly larger than respiration causing net autotrophy ($\mathrm{NCP} > 0$) and summer respiration is slightly larger than productivity causing net heterotrophy ($\mathrm{NCP} < 0$). The same cycle occurs again in the late summer/early fall, with a shorter time period of primary production exceeding respiration (net autotrophy) followed by a time during which respiration exceeded primary production (net heterotrophy).

Interannual variability of NCP was also substantial (Figure 9), due to large interannual variations in DIN transport into the MAB. Riverine fluxes along the U.S. East Coast vary substantially from year to year in response to variability in rates of precipitation and evapotranspiration (Yang, Tian, Friedrichs, Hopkinson, et al., 2015; Yang, Tian, Friedrichs, Liu, et al., 2015). Although the interannual variability of riverine DIN inputs may be significant, that is, nearly a factor of 2 different between 2004 (0.15 Tg N/year) and 2007 (0.08 Tg N/year; Table 3), the interannual difference (Δ = 0.07 Tg N/year) is much less than the interannual difference of DIN entering along the shelf from the northeast (Δ = 0.56 Tg N/year) and flowing across the continental slope (Δ = 1.00 Tg N/year). However, the interannual variability of the sum of these two fluxes (across slope + along shelf) is smaller than either individually, since in each year the large volume flux entering from the northeast (5-year mean = 80 mSv; Table 1) is nearly balanced by the large volume flux leaving the MAB across the continental slope (5-year mean = 87 mSv; Table 1). Nevertheless, the interannual variability of the net advective flux to the MAB (across slope + along shelf) is still larger than that entering from the estuaries and rivers both in terms of DIN inputs and water volume flux.

The large interannual variability in along-shelf and across-shelf transport in the MAB is well known (e.g., He et al., 2011) and is ultimately responsible for the interannual variability in NCP (Figure 9). Somewhat surprisingly, NCP is highest in the year that the water volume flux entering from the estuaries and rivers is lowest (2007), indicating that the main source of DIN for the high NCP is not terrestrial. For the years studied here (2004–2008), low estuarine and riverine input of water to the MAB cooccurs with the greatest input of water across the continental slope in the southern MAB (Figure 6e and Table 1). Specifically, NCP is highest in the years when the Gulf Stream is situated closest to the MAB (2007 and 2008), remaining along the continental slope longer relative to other years before heading out to the open ocean (Figures 8e and 8f) and thus providing greater opportunity for onshore intrusions of offshore waters through warm core rings that develop from Gulf Stream meanders and other shelf break exchange processes (Gawarkiewicz et al., 1996; Kang & Curchitser, 2015; Lentz, 2003; W. G. Zhang et al., 2013; W. G. Zhang & Gawarkiewicz, 2015; S. Zhang et al., 2018). The unusually close proximity of the warm Gulf Stream waters to the continental slope in these particular years (2007–2008) is evident from satellite-derived sea surface temperatures showing unusually warm MAB waters (Figures 11a and 11c), in close agreement with the model results (Figures 11b and 11d). The literature also provides other examples of onshore excursions of the Gulf Stream at the southern end of the MAB. For example, using sea surface temperatures and hydrographic data, Churchill and Cornillon (1991)

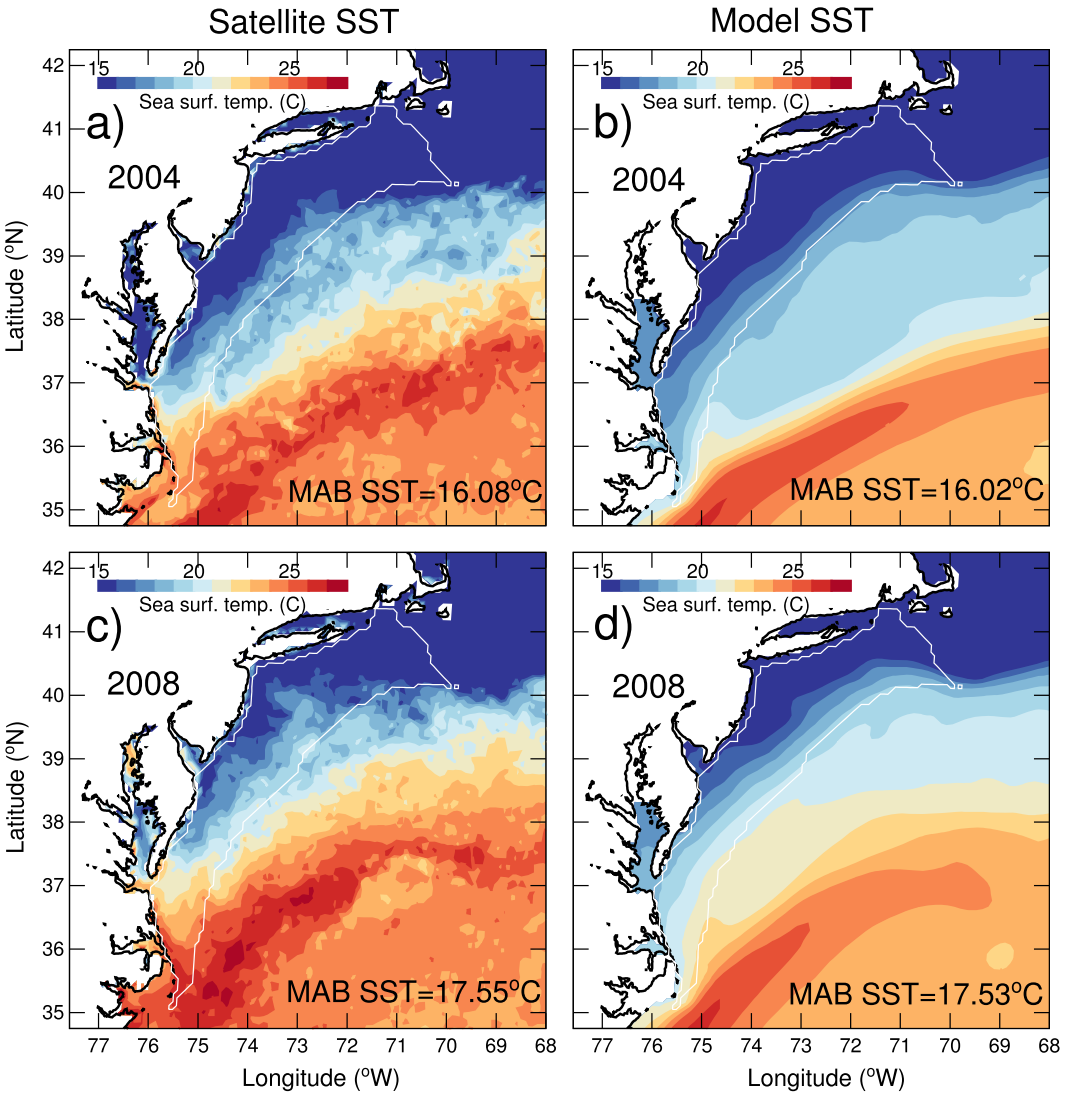

Figure 11. Comparison of annually averaged sea surface temperature for 2004 (a, b) and 2008 (c, d) from satellite-derived data (a, c; NODC and Rosenstiel School of Marine and Atmospheric Science, 2003) and from the USECoS model (b, d). Both the satellite data and model results show a closer impingement of the Gulf Stream on the southern MAB shelf in 2008, compared to 2004. SST = sea surface temperature; MAB = Mid-Atlantic Bight.

tracked such excursions and documented the presence of Gulf Stream water on the continental shelf 80–300 km north of Cape Hatteras. Similarly, Biscaye et al. (1994) show a large northward excursion of the Gulf Stream occurring during the SEEP-II experiment in 1988–1989. Overall, our results showing that broad-scale circulation patterns are significant drivers of ecosystem variability are consistent with other studies that have demonstrated that fluctuations in water masses and circulation patterns drive shifts in ecosystem states (Nye et al., 2014). However, a longer model simulation would be required to determine whether there is a significant inverse correlation between water transported into the MAB from the rivers and estuaries, and water entering the southern MAB across the continental slope.

4.3. Future Modeling Efforts

The advantages of the modeling system used in this study relative to those used in earlier model-based analyses of MAB nitrogen budgets are as follows: (1) linkages with a sophisticated mechanistic terrestrial model (DLEM; Tian et al., 2015; Yang, Tian, Friedrichs, Hopkinson, et al., 2015); Yang, Tian, Friedrichs, Liu, et al., 2015 that provides riverine inputs of freshwater and nitrogen, (2) linkages with the CMAQ model that provides

atmospheric inputs of nitrogen (St-Laurent et al., 2017), and (3) a more realistic biogeochemical model that includes multiple phytoplankton and zooplankton size classes (Xiao & Friedrichs, 2014a) as well as dissolved organic matter, resuspension, and burial (Druon et al., 2010). However, this modeling system can be improved by better representation of the estuaries and inclusion of data assimilation, each of which is discussed below.

Estuaries are key regions of biogeochemical transformations of inorganic and organic nitrogen. Although the regional model used here resolves the U.S. East Coast estuaries to some degree (Figure 1), the horizontal resolution of the grid prohibits adequate resolution of the complex coastline and critical bathymetric gradients inside these estuaries, which are critical for correctly representing both physical and biogeochemical processes (Ye et al., 2018). For example, the lack of a deep mainstem trench in the Chesapeake Bay prevents the development of hypoxia and hence water column denitrification, which is a key biogeochemical transformation process in the estuary (Da et al., 2018; Feng et al., 2015; Irby et al., 2018, 2016; Wiggert et al., 2017). The version of the USECoS biogeochemical model used here also neglects inorganic sediment inputs from the rivers, which can significantly affect light attenuation and therefore estuarine productivity. Specifically, better spatial resolution of the estuarine physical and biogeochemical processes will alleviate overestimating the input of inorganic nitrogen to the MAB and underestimating the input of organic nitrogen. Using a higher-resolution Chesapeake Bay hydrodynamic-biogeochemical model, Feng et al. (2015) found an order of magnitude more DIN entering the Chesapeake Bay via rivers than exiting through the bay mouth to the MAB. They contrasted their results with those of a lower-resolution model without estuarine-specific biogeochemical processes such as water column denitrification and light attenuation due to inorganic suspended sediment. The lower-resolution model quickly transported riverine nutrients directly to the shelf, so there was no time for extensive remineralization of the nutrients within the estuarine system. As a result, riverine inputs of DIN and coastal exports of DIN were much more similar in magnitude for the low-resolution model. Results from our analyses suggest that the modeling system used here is likewise overestimating the input of DIN to the continental shelf, likely again because of underestimating estuarine residence times and neglecting critical estuarine processes. Ongoing work is focused on implementing a nested higher-resolution grid in the east coast estuaries, implementing estuarine-specific processes such as water column denitrification and inorganic sediment inputs, and examining the impact on the nitrogen budget.

Assimilation of biogeochemical observations, either in situ or remotely sensed, provides an approach for improving simulations of nutrient and carbon budgets (Friedrichs & Kaufman, 2018; Hofmann & Friedrichs, 2001; Kaufman et al., 2018; Xiao & Friedrichs, 2014a, 2014b). Perhaps more importantly, assimilation of physical data using a variational data assimilation algorithm will help ensure that the space and time structure of the MAB circulation is consistent with available observations and includes the details of the regional circulation (Levin et al., 2018). In particular, assimilating physical data such as temperature, salinity, and sea surface height anomalies will improve the realism of the model simulations by adjusting the positions of the Gulf Stream and associated mesoscale eddies (Kang & Curchitser, 2013) closer to their observed locations. Since a key result of this paper is that nitrogen fluxes are highly dependent on the MAB circulation field, it is important to accurately represent the circulation of the MAB when attempting to quantify these fluxes.

5. Summary and Conclusions

Continental shelves are characterized by complex physical and biological processes occurring at a variety of temporal and spatial scales, making it difficult to acquire enough observations to fully resolve area-integrated annual nitrogen fluxes for shelf regions. Here a 3-D coupled biogeochemical-circulation model was applied to the MAB to investigate the nitrogen budget of this region and examine the spatiotemporal variability of key nitrogen fluxes. NCP was characterized by strong spatial, seasonal, and interannual variability, especially when compared to other biogeochemical nitrogen fluxes such as burial and denitrification. The strong interannual variability of NCP was not directly due to interannual variability of terrestrial inorganic nitrogen inputs but rather was due to interannual variability in oceanic circulation patterns, which caused significant changes in the along-shelf and across-slope horizontal fluxes transporting water into and out of the MAB. Typically, horizontal water transport and inorganic nitrogen flux entered the MAB from the northeast and exited the MAB along the continental slope. However, when a meander caused the Gulf

Stream to remain along the continental slope longer before veering out to the open ocean, intrusions of deep high nutrient water onto the shelf stimulated productivity and increased NCP. In this way oceanic circulation patterns were found to drive NCP variability to a greater degree than interannually varying terrestrial inputs of inorganic nitrogen.

The modeling system used here has been evaluated with in situ and satellite data (St-Laurent et al., 2017) and includes substantial improvements over earlier MAB models (Cahill et al., 2016) including linkages with a sophisticated terrestrial model, an air-quality model, and a more realistic biogeochemical model. However, significant improvements are already underway, including an increased resolution in the estuaries through nesting, assimilation of physical data to improve the realism of circulation patterns, and longer simulations to further test the results found here for the 5-year analysis. Overall, the strong spatiotemporal variability in nitrogen fluxes reported here highlights the importance of the breadth of data coverage throughout all seasons and across multiple years in order to correctly assess the current status and future changes in the MAB nitrogen budget.

Acknowledgments
This work was supported by NASA Headquarters under the NASA Earth and Space Science Fellowship Program (NNX10AN50H) and the NASA Interdisciplinary Science Program (NNX11AD47G and NNX14AF93G). D.A. Narvaez is partially funded by COPAS Sur-Austral CONICYT PIA APOYO CCTE AFB170006 and FONDECYT 1116109. This work was performed using High Performance Computing facilities at the College of William & Mary, which were provided by contributions from the National Science Foundation, the Commonwealth of Virginia Equipment Trust Fund and the Office of Naval Research. We would also like to thank the two anonymous reviewers for their very helpful comments and suggestions. Model output is publicly available through W&M's ScholarWorks at (https://doi.org/10.25773/2f36-pn56). This paper is contribution 3793 of the Virginia Institute of Marine Science, College of William and Mary.

References

Appel, K. W., Foley, K. M., Bash, J. O., Pinder, R. W., Dennis, R. L., Allen, D. J., & Pickering, K. (2011). A multi-resolution assessment of the Community Multiscale Air Quality (CMAQ) model v4.7 wet deposition estimates for 2002-2006. *Geoscientific Model Development*, *4*(2), 357–371. https://doi.org/10.5194/gmd-4-357-2011

Biscaye, P. E., Flagg, C. N., & Falkowski, P. G. (1994). The shelf edge exchanges processes experiment, SEEP-II: An introduction to hypotheses, results and conclusions. *Deep Sea Research, Part II*, *41*(2-3), 231–252. https://doi.org/10.1016/0967-0645(94)90022-1

Blanton, J. O., Atkinson, L. P., Pietrafesa, L. J., & Lee, T. N. (1981). The intrusion of Gulf Stream water across the continental shelf due to topographically-induced upwelling. *Deep Sea Research Part A*, *28*(4), 393–405. https://doi.org/10.1016/0198-0149(81)90006-6

Caesar, L., Rahmstorf, S., Robinson, A., Feulner, G., & Saba, V. (2018). Observed fingerprint of a weakening Atlantic Ocean overturning circulation. *Nature*, *556*(7700), 191–196. https://doi.org/10.1038/s41586-018-0006-5

Cahill, B., Wilkin, J., Fennel, K., Vandemark, D., & Friedrichs, M. A. M. (2016). Interannual and seasonal variabilities in air-sea CO_2 fluxes along the U.S. eastern continental shelf and their sensitivity to increasing air temperatures and variable winds. *Journal of Geophysical Research: Biogeosciences*, *121*, 295–311. https://doi.org/10.1002/2015JG002939

Carlson, C. A., Hansell, D. A., Nelson, N. B., Siegel, D. A., Smethie, W. M., Khatiwala, S., et al. (2010). Dissolved organic carbon export and subsequent remineralization in the mesopelagic and bathypelagic realms of the North Atlantic basin. *Deep-Sea Research Part II-Topical Studies in Oceanography*, *57*(16), 1433–1445. https://doi.org/10.1016/j.dsr2.2010.02.013

Chassignet, E. P., Hurlburt, H. E., Smedstad, O. M., Halliwell, G. R., Hogan, P. J., Wallcraft, A. J., et al. (2007). The HYCOM (HYbrid Coordinate Ocean Model) data assimilative system. *Journal of Marine Systems*, *65*(1–4), 60–83. https://doi.org/10.1016/j.jmarsys.2005.09.016

Chen, C. T. A., Liu, K. K., & Macdonald, R. (2003). Continental margin exchanges. In M. J. R. Fasham (Ed.), *Ocean Biogeochemistry: A JGOFS Synthesis* (pp. 53–97). Berlin: Springer. https://doi.org/10.1007/978-3-642-55844-3_4

Chen, K., Gawarkiewicz, G., Kwon, Y.-O., & Zhang, W. G. (2015). The role of atmospheric forcing versus ocean advection during the extreme warming of the northeast U.S. continental shelf in 2012. *Journal of Geophysical Research: Oceans*, *120*, 4324–4339. https://doi.org/10.1002/2014JC010547

Chen, K., & He, R. (2015). Mean circulation in the coastal ocean off northeastern North America from a regional-scale ocean model. *Ocean Science*, *11*(4), 503–517. https://doi.org/10.5194/os-11-503-2015

Chen, K., He, R., Powell, B. S., Gawarkiewicz, G. G., Moore, A. M., & Arango, H. G. (2014). Data assimilative modeling investigation of Gulf Stream Warm Core Ring interaction with continental shelf and slope circulation. *Journal of Geophysical Research: Oceans*, *119*, 5968–5991. https://doi.org/10.1002/2014JC009898

Chen, K., & Kwon, Y.-O. (2018). Does Pacific variability influence the Northwest Atlantic shelf temperature? *Journal of Geophysical Research: Oceans*, *123*, 4110–4131. https://doi.org/10.1029/2017JC013414

Churchill, J. H., & Cornillon, P. C. (1991). Gulf Stream water on the shelf and upper slope north of Cape Hatteras. *Continental Shelf Research*, *11*(5), 409–431. https://doi.org/10.1016/0278-4343(91)90051-7

Csanady, G. T., & Hamilton, P. (1988). Circulation of slopewater. *Continental Shelf Research*, *8*(5-7), 565–624. https://doi.org/10.1016/0278-4343(88)90068-4

Da, F., Friedrichs, M. A. M., & St-Laurent, P. (2018). Impacts of atmospheric nitrogen deposition and coastal nitrogen fluxes on oxygen concentrations in Chesapeake Bay. *Journal of Geophysical Research: Oceans*, *123*, 5004–5025. https://doi.org/10.1029/2018JC014009

Druon, J. N., Mannino, A., Signorini, S., McClain, C., Friedrichs, M. A. M., Wilkin, J., & Fennel, K. (2010). Modeling the dynamics and export of dissolved organic matter in the northeastern US continental shelf. *Estuarine, Coastal and Shelf Science*, *88*(4), 488–507. https://doi.org/10.1016/j.ecss.2010.05.010

Ezer, T. (2015). Detecting changes in the transport of the Gulf Stream and the Atlantic overturning circulation from coastal sea level data: The extreme decline in 2009–2010 and estimated variations for 1935-2012. *Global and Planetary Change*, *129*, 23–36. https://doi.org/10.1016/j.gloplacha.2015.03.002

Fairall, C. W., Bradley, E. F., Hare, J. E., Grachev, A. A., & Edson, J. B. (2003). Bulk parameterization of air-sea fluxes: Updates and verification for the COARE algorithm. *Journal of Climate*, *16*(4), 571–591. https://doi.org/10.1175/1520-0442(2003)016<0571:bpoasf>2.0.co;2

Fasham, M. J. R., Boyd, P. W., & Savidge, G. (1999). Modeling the relative contributions of autotrophs and heterotrophs to carbon flow at a Lagrangian JGOFS station in the Northeast Atlantic: The importance of DOC. *Limnology and Oceanography*, *44*(1), 80–94. https://doi.org/10.4319/lo.1999.44.1.0080

Feng, Y., Friedrichs, M. A. M., Wilkin, J., Tian, H., Yang, Q., Hofmann, E. E., et al. (2015). Chesapeake Bay nitrogen fluxes derived from a land-estuarine ocean biogeochemical modeling system: Model description, evaluation, and nitrogen budgets. *Journal of Geophysical Research: Biogeosciences*, *120*, 1666–1695. https://doi.org/10.1002/2015JG002931

Fennel, K. (2010). The role of continental shelves in nitrogen and carbon cycling: Northwestern North Atlantic case study. *Ocean Science*, *6*(2), 539–548. https://doi.org/10.5194/os-6-539-2010

Fennel, K., Wilkin, J., Levin, J., Moisan, J., O'Reilly, J., & Haidvogel, D. (2006). Nitrogen cycling in the Middle Atlantic Bight: Results from a three-dimensional model and implications for the North Atlantic nitrogen budget. *Global Biogeochemical Cycles*, *20*, GB3007. https://doi.org/10.1029/2005GB002456

Fennel, K., Wilkin, J., Previdi, M., & Najjar, R. G. (2008). Denitrification effects on air-sea CO_2 flux in the coastal ocean: Simulations for the Northwest North Atlantic. *Geophysical Research Letters*, *35*, L24608. https://doi.org/10.1029/2008GL036147

Filippino, K. C., Mulholland, M. R., & Bernhardt, P. W. (2011). Nitrogen uptake and primary productivity rates in the Mid-Atlantic Bight (MAB). *Estuarine, Coastal and Shelf Science*, *91*(1), 13–23. https://doi.org/10.1016/j.ecss.2010.10.001

Friedrichs, M. A. M., & Kaufman, D. E. (2018). In A. Schiller, & G. Brassington (Eds.), *Marine biogeochemical data assimilation*, Reference Module in Earth Systems and Environmental Sciences. Dordrecht, Netherlands: Springer. https://doi.org/10.1016/B978-0-12-409548-9.11261-8

Galloway, J. N., Dentener, F. J., Capone, D. G., Boyer, E. W., Howarth, R. W., Seitzinger, S. P., et al. (2004). Nitrogen cycles: Past, present, and future. *Biogeochemistry*, *70*(2), 153–226. https://doi.org/10.1007/s10533-004-0370-0

Gantt, B., Kelly, J. T., & Bash, J. (2015). Updating sea spray aerosol emissions in the Community Multiscale Air Quality (CMAQ) model version 5.0.2. *Geoscientific Model Development*, *8*(11), 3733–3746. https://doi.org/10.5194/gmd-8-3733-2015

Garcia, H. E., Locarnini, R. A., Boyer, T. P., Antonov, J. I., Baranova, O. K., Zweng, M. M., et al. (2014a). In S. Levitus & A. Mishonov (Eds.), *World Ocean Atlas 2013, volume 4: Dissolved inorganic nutrients (phosphate, nitrate, silicate), NOAA Atlas NESDIS* (Vol. 76, p. 25).

Garcia, H. E., Locarnini, R. A., Boyer, T. P., Antonov, J. I., Baranova, O. K., Zweng, M. M., et al. (2014b). In S. Levitus & A. Mishonov (Eds.), *World Ocean Atlas 2013, volume 3: Dissolved oxygen, apparent oxygen utilization, and oxygen saturation, NOAA Atlas NESDIS* (Vol. 75, p. 27).

Gawarkiewicz, G., Ferdelman, T., Church, T. M., & Luther, G. W. (1996). Shelfbreak frontal structure on the continental shelf north of Cape Hatteras. *Continental Shelf Research*, *16*(14), 1751–1773. https://doi.org/10.1016/0278-4343(96)00014-3

Hansell, D. A., & Carlson, C. A. (2001). Marine dissolved organic matter and the carbon cycle. *Oceanography*, *14*(4), 41–49. https://doi.org/10.5670/oceanog.2001.05

Harding, L. W. Jr., Mallonee, M. E., & Perry, E. S. (2002). Toward a predictive understanding of primary productivity in a temperate, partially stratified estuary. *Estuarine, Coastal and Shelf Science*, *55*(3), 437–463. https://doi.org/10.1006/ecss.2001.0917

He, R., Chen, K., Fennel, K., Gawarkiewicz, G., & McGillicuddy, D. (2011). Seasonal and interannual variability of physical and biological dynamics at the shelfbreak front of the Middle Atlantic Bight: Nutrient supply mechanisms. *Biogeosciences*, *8*(1), 1555–1590. https://doi.org/10.5194/bgd-8-1555-2011

Hermann, A. J., Hinckley, S., Dobbins, E. L., Haidvogel, D. B., Bond, N. A., Mordy, C., et al. (2009). Quantifying cross-shelf and vertical nutrient flux in the Coastal Gulf of Alaska with a spatially nested, coupled biophysical model. *Deep Sea Research Part II: Topical Studies in Oceanography*, *56*(24), 2474–2486. https://doi.org/10.1016/j.dsr2.2009.02.008

Herrmann, M., Najjar, R. G., Kemp, W. M., Alexander, R. B., Boyer, E. W., Cai, W.-J., et al. (2015). Net ecosystem production and organic carbon balance of U.S. East Coast estuaries: A synthesis approach. *Global Biogeochemical Cycles*, *29*, 96–111. https://doi.org/10.1002/2013GB004736

Hofmann, E. E., Cahill, B., Fennel, K., Friedrichs, M. A. M., Hyde, K., Lee, C., et al. (2011). Modeling the dynamics of continental shelf carbon. *Annual Review of Marine Science*, *3*(1), 93–122. https://doi.org/10.1146/Annurev-Marine-120709-142740

Hofmann, E. E., Druon, J.-N., Fennel, K., Friedrichs, M. A. M., Haidvogel, D., Lee, C., et al. (2008). Eastern US continental shelf carbon budget integrating models, data assimilation, and analysis. *Oceanography*, *21*(1), 86–104. https://doi.org/10.5670/oceanog.2008.70

Hofmann, E. E., & Friedrichs, M. A. M. (2001). Biogeochemical data assimilation. In J. H. Steele, S. A. Thorpe, & K. K. Turekian (Eds.), *Encyclopedia of Ocean Sciences* (Vol. 1, pp. 302–308). London, UK: Academic Press.

Hopkinson, C. S., & Vallino, J. J. (2005). Efficient export of carbon to the deep ocean through dissolved organic matter. *Nature*, *433*(7022), 142–145. https://doi.org/10.1038/nature03191

Irby, I. D., Friedrichs, M. A. M., Da, F., & Hinson, K. E. (2018). The competing impacts of climate change and nutrient reductions on dissolved oxygen in Chesapeake Bay. *Biogeosciences*, *15*(9), 2649–2668. https://doi.org/10.5194/bg-15-2649-2018

Irby, I. D., Friedrichs, M. A. M., Friedrichs, C. T., Bever, A. J., Hood, R. R., Lanerolle, L. W. J., et al. (2016). Challenges associated with modeling low-oxygen waters in Chesapeake Bay: A multiple model comparison. *Biogeosciences*, *13*(7), 2011–2028. https://doi.org/10.5194/bg-13-2011-2016

Jahnke, R. A. (2010). Chapter 16: Global synthesis. In K. K. Liu, L. Atkinson, R. Quinones, & L. Talaue-McManus (Eds.), *Carbon and nutrient fluxes in continental margins* (pp. 597–615). New York: Springer-Verlag. https://doi.org/10.1007/978-3-540-92735-8_16

Ji, R. B., Davis, C. S., Chen, C. S., Townsend, D. W., Mountain, D. G., & Beardsley, R. C. (2007). Influence of ocean freshening on shelf phyto-plankton dynamics. *Geophysical Research Letters*, *34*, L24607. https://doi.org/10.1029/2007GL032010

Kang, D., & Curchitser, E. N. (2013). Gulf Stream eddy characteristics in a high-resolution ocean model. *Journal of Geophysical Research: Oceans*, *118*, 4474–4487. https://doi.org/10.1002/jgrc.20318

Kang, D., & Curchitser, E. N. (2015). Energetics of eddy-mean flow interactions in the Gulf Stream region. *Journal of Physical Oceanography*, *45*(4), 1103–1120. https://doi.org/10.1175/JPO-D-14-0200.1

Kaufman, D. E., Friedrichs, M. A. M., Hemmings, J. C. P., & Smith, W. O. Jr. (2018). Assimilating bio-optical glider data during a phytoplankton bloom in the southern Ross Sea. *Biogeosciences*, *15*(1), 73–90. https://doi.org/10.5194/bg-15-73-2018

Kishi, M. J., Kashiwai, M., Ware, D. M., Megrey, B. A., Eslinger, D. L., Werner, F. E., et al. (2007). NEMURO—A lower trophic level model for the North Pacific marine ecosystem. *Ecological Modelling*, *202*(1-2), 12–25. https://doi.org/10.1016/j.ecolmodel.2006.08.021

Kuring, N., Lewis, M. R., Platt, T., & O'Reilly, J. E. (1990). Satellite-derived estimates of primary production on the northwest Atlantic continental shelf. *Continental Shelf Research*, *10*(5), 461–484. https://doi.org/10.1016/0278-4343(90)90050-V

Laursen, A. E., & Seitzinger, S. P. (2002). The role of denitrification in nitrogen removal and carbon mineralization in Mid-Atlantic Bight sediments. *Continental Shelf Research*, *22*(9), 1397–1416. https://doi.org/10.1016/S0278-4343(02)00008-0

Lentz, S. J. (2003). A climatology of salty intrusions over the continental shelf from Georges Bank to Cape Hatteras. *Journal of Geophysical Research*, *108*(C10), 3326. https://doi.org/10.1029/2003JC001859

Lentz, S. J. (2008a). Observations and a model of the mean circulation over the Middle Atlantic Bight continental shelf. *Journal of Physical Oceanography*, *38*(6), 1203–1221. https://doi.org/10.1175/2007JPO3768.1

Lentz, S. J. (2008b). Seasonal variations in the circulation over the Middle Atlantic Bight continental shelf. *Journal of Physical Oceanography*, *38*(7), 1486–1500. https://doi.org/10.1175/2007JPO3767.1

Levin, J., Wilkin, J., Fleming, N., & Zavala-Garay, J. (2018). Mean circulation of the Mid-Atlantic Bight from a climatological data assimilative model. *Ocean Modelling*, *128*, 1–14. https://doi.org/10.1016/j.ocemod.2018.05.003

Linder, C. A., & Gawarkiewicz, G. (1998). A climatology of the shelf break front in the middle Atlantic bight. *Journal of Geophysical Research*, *103*(C9), 18,405–18,423. https://doi.org/10.1029/98JC01438

Linder, C. A., Gawarkiewicz, G. G., & Taylor, M. (2006). Climatological estimation of environmental uncertainty over the Middle Atlantic Bight shelf and slope. *IEEE Journal of Oceanic Engineering*, *31*(2), 308–324. https://doi.org/10.1109/JOE.2006.877145

Lozier, M. S., & Gawarkiewicz, G. (2001). Cross-frontal exchange in the Middle Atlantic Bight as evidenced by surface drifters. *Journal of Physical Oceanography*, *31*(8), 2498–2510. https://doi.org/10.1175/1520-0485(2001)031<2498:CFEITM>2.0.CO;2

Mahadevan, A., & Archer, D. (2000). Modeling the impact of fronts and mesoscale circulation on the nutrient supply and biogeochemistry of the upper ocean. *Journal of Geophysical Research*, *105*(C1), 1209–1225. https://doi.org/10.1029/1999JC900216

Mannino, A., Signorini, S. R., Novak, M. G., Wilkin, J., Friedrichs, M. A. M., & Najjar, R. G. (2016). Dissolved organic carbon fluxes in the Middle Atlantic Bight: An integrated approach based on satellite data and ocean model products. *Journal of Geophysical Research: Biogeosciences*, *121*, 312–336. https://doi.org/10.1002/2015JG00303

McGillicuddy, D. J., Robinson, A. R., Siegel, D. A., Jannasch, H. W., Johnsonk, R., Dickey, T. D., et al. (1998). Influence of mesoscale eddies on new production in the Sargasso Sea. *Nature*, *394*(6690), 263–266. https://doi.org/10.1038/28367

Mellor, G. L., & Yamada, T. (1982). Development of a turbulence closure model for geophysical fluid problems. *Reviews of Geophysics and Space Physics*, *20*(4), 851–875. https://doi.org/10.1029/RG020i004p00851

Mesinger, F., DiMego, G., Kalnay, E., Mitchell, K., Shafran, P. C., Ebisuzaki, W., et al. (2006). North American Regional Reanalysis: A long-term, consistent, high-resolution climate dataset for the North American domain, as a major improvement upon the earlier global reanalysis datasets in both resolution and accuracy. *Bulletin of the American Meteorological Society*, *87*(3), 343–360. https://doi.org/10.1175/BAMS-87-3-343

Mulholland, M. R., Bernhardt, P. W., Blanco-Garcia, J. L., Mannino, A., Hyde, K., Mondragon, E., et al. (2012). Rates of dinitrogen fixation and the abundance of diazotrophs in North American coastal waters between Cape Hatteras and Georges Bank. *Limnology and Oceanography*, *57*(4), 1067–1083. https://doi.org/10.4319/lo.2012.57.4.1067

Muller-Karger, F. E., Varela, R., Thunell, R., Luerssen, R., Hu, C. M., & Walsh, J. J. (2005). The importance of continental margins in the global carbon cycle. *Geophysical Research Letters*, *32*, L01602. https://doi.org/10.1029/2004GL021346

Najjar, R. G., Herrmann, M., Alexander, R., Boyer, E. W., Burdige, D. J., Butman, D., et al. (2018). Carbon budget of tidal wetlands, estuaries, and shelf waters of eastern North America. *Global Biogeochemical Cycles*, *32*, 389–416. https://doi.org/10.1002/2017GB005790

National Aeronautics and Space Administration (2014). SeaWiFS level-3 standard mapped image at 9 km resolution (OC4 algorithm), NASA Goddard Space Flight Center, Ocean Ecology Laboratory, Ocean Biology Processing Group.

NODC and Rosenstiel School of Marine and Atmospheric Science (2003). AVHRR Pathfinder Level 3 Monthly Nighttime SST Version 5. PO.DAAC, CA, USA. Dataset accessed 2018-09-29. https://doi.org/10.5067/PATHF-MON50

Nye, J. A., Baker, M. R., Bell, R., Kenny, A., Kilbourne, K. H., Friedland, K. D., et al. (2014). Ecosystem effects of the Atlantic Multidecadal Oscillation. *Journal of Marine Systems*, *133*, 103–116. https://doi.org/10.1016/j.jmarsys.2013.02.006

O'Reilly, J., Evans-Zetlin, C. E., & Busch, D. A. (1987). Primary production. In R. H. Backus (Ed.), *Georges Bank* (pp. 220–233). Cambridge, MA: MIT Press.

Oschlies, A., & Garcon, V. (1998). Eddy-induced enhancement of primary production in a model of the North Atlantic Ocean. *Nature*, *394*(6690), 266–269. https://doi.org/10.1038/28373

Ryan, J. P., Yoder, J. A., & Cornillon, P. C. (1999). Enhanced chlorophyll at the shelfbreak of the Mid-Atlantic Bight and Georges Bank during the spring transition. *Limnology and Oceanography*, *44*(1), 1–11. https://doi.org/10.4319/lo.1999.44.1.0001

Saba, V. S., Griffies, S. M., Anderson, W. G., Winton, M., Alexander, M. A., Delworth, T. L., et al. (2016). Enhanced warming of the Northwest Atlantic Ocean under climate change. *Journal of Geophysical Research: Oceans*, *121*, 118–132. https://doi.org/10.1002/2015JC011346

Sasai, Y., Ishida, A., Sasaki, H., Kawahara, S., Uehara, H., & Yamanaka, Y. (2006). A global eddy-resolving coupled physical-biological model: Physical influences on a marine ecosystem in the North Pacific. *Simulation-Transactions of the Society for Modeling and Simulation International*, *82*(7), 467–474. https://doi.org/10.1177/0037549706068943

Schollaert, S. E., Rossby, T., & Yoder, J. A. (2004). Gulf stream cross-frontal exchange: Possible mechanisms to explain interannual variations in phytoplankton chlorophyll in the Slope Sea during the SeaWiFS years. *Deep Sea Research Part II: Topical Studies in Oceanography*, *51*(1–3), 173–188. https://doi.org/10.1016/j.dsr2.2003.07.017

Schrum, C., Alekseeva, I., & St John, M. (2006). Development of a coupled physical-biological ecosystem model ECOSMO—Part I: Model description and validation for the North Sea. *Journal of Marine Systems*, *61*(1–2), 79–99. https://doi.org/10.1016/j.jmarsys.2006.01.005

Schulte, J. A., Georgas, N., Saba, V., & Howell, P. (2018). North Pacific influences on Long Island sound temperature variability. *Journal of Climate*, *31*(7), 2745–2769. https://doi.org/10.1175/JCLI-D-17-0135

Seitzinger, S. P., & Giblin, A. E. (1996). Estimating denitrification in North Atlantic continental shelf sediments. *Biogeochemistry*, *35*(1), 235–260. https://doi.org/10.1007/bf02179829

Shchepetkin, A. F., & McWilliams, J. C. (2005). The regional oceanic modeling system (ROMS): A split-explicit, free-surface, topography-following-coordinate oceanic model. *Ocean Modelling*, *9*(4), 347–404. https://doi.org/10.1016/j.ocemod.2004.08.002

Shenk, G. W., & Linker, L. C. (2013). Development and application of the 2010 Chesapeake Bay watershed total maximum daily load model. *Journal of the American Water Resources Association*, *49*, 1042–1056.

Siegel, D. A., McGillicuddy, D. J., & Fields, E. A. (1999). Mesoscale eddies, satellite altimetry, and new production in the Sargasso Sea. *Journal of Geophysical Research*, *104*(C6), 13,359–13,379. https://doi.org/10.1029/1999JC900051

Smolarkiewicz, P. K., & Margolin, L. G. (1998). MPDATA: A finite difference solver for geophysical flows. *Journal of Computational Physics*, *140*(2), 459–480. https://doi.org/10.1006/jcph.1998.5901

St-Laurent, P., Friedrichs, M. A. M., Najjar, R. G., Martins, D. K., Herrmann, M., Miller, S. K., & Wilkin, J. (2017). Impacts of atmospheric nitrogen deposition on surface waters of the western North Atlantic mitigated by multiple feedbacks. *Journal of Geophysical Research: Oceans*, *122*, 8406–8426. https://doi.org/10.1002/2017JC013072

Tian, H., Chen, G., Liu, M., Zhang, C., Sun, G., Lu, C., et al. (2010). Model estimates of ecosystem net primary productivity, evapotranspiration, and water use efficiency in the southern United States during 1895–2007. *Forest Ecology and Management*, *259*(7), 1311–1327. https://doi.org/10.1016/j.foreco.2009.10.009

Tian, H., Yang, Q., Najjar, R. G., Ren, W., Friedrichs, M. A. M., Hopkinson, C. S., & Pan, S. (2015). Anthropogenic and climatic influences on carbon fluxes from eastern North America to the Atlantic Ocean: A process-based modeling study. *Journal of Geophysical Research: Biogeosciences*, *120*, 757–772. https://doi.org/10.1002/2014JG002760

Wakelin, S. L., Holt, J. T., Blackford, J. C., Allen, J. I., Butenschön, M., & Artioli, Y. (2012). Modeling the carbon fluxes of the northwest European continental shelf: Validation and budgets. *Journal of Geophysical Research*, *117*, C05020. https://doi.org/10.1029/2011JC007402

Wiggert, J. D., Hood, R. R., & Brown, C. W. (2017). Modeling Hypoxia and Its Ecological Consequences in Chesapeake Bay. In D. Justic, K. Rose, R. Hetland, & K. Fennel (Eds.), *Modeling Coastal Hypoxia*. Cham: Springer.

Wilkin, J. L. (2006). The summertime heat budget and circulation of southeast new England shelf waters. *Journal of Physical Oceanography*, *36*(11), 1997–2011. https://doi.org/10.1175/jpo2968.1

Xiao, Y., & Friedrichs, M. A. M. (2014a). Using biogeochemical data assimilation to assess the relative skill of multiple ecosystem models in the Mid-Atlantic Bight: Effects of increasing the complexity of the planktonic food web. *Biogeosciences*, *11*(11), 3015–3030. https://doi.org/10.5194/bg-11-3015-2014

Xiao, Y., & Friedrichs, M. A. M. (2014b). The assimilation of satellite-derived data into a one-dimensional lower trophic level marine ecosystem model. *Journal of Geophysical Research: Oceans*, *119*, 2691–2712. https://doi.org/10.1002/2013JC009433

Xu, Y., Cahill, B., Wilkin, J., & Schofield, O. (2013). Role of wind in regulating phytoplankton blooms on the Mid-Atlantic Bight. *Contiental Shelf Research*, *63*, S26–S35. https://doi.org/10.1016/j.csr.2012.09.011

Xue, Z., He, R., Fennel, K., Cai, W.-J., Lohrenz, S., & Hopkinson, C. (2013). Modeling ocean circulation and biogeochemical variability in the Gulf of Mexico. *Biogeosciences*, *10*(11), 7219–7234. https://doi.org/10.5194/bg-10-7219-2013

Yang, Q., Tian, H., Friedrichs, M. A. M., Hopkinson, C. S., Lu, C., & Najjar, R. G. (2015). Increased nitrogen export from eastern North America to the Atlantic Ocean due to climatic and anthropogenic changes during 1901-2008. *Journal of Geophysical Research: Biogeosciences*, *120*, 1046–1068. https://doi.org/10.1002/2014JG002763

Yang, Q., Tian, H., Friedrichs, M. A. M., Liu, M., Li, X., & Yang, J. (2015). Hydrological responses to climate and land-use changes along the North American east coast: A 110-year historical reconstruction. *Journal of the American Water Resources Association*, *51*(1), 47–67. https://doi.org/10.1111/jawr.12232

Ye, F., Zhang, Y. J., Wang, H. V., Friedrichs, M. A. M., Irby, I. D., Alteljevich, E., et al. (2018). A 3D unstructured-grid model for the Chesapeake Bay: Importance of bathymetry. *Ocean Modelling*, *127*, 16–39. https://doi.org/10.1016/j.ocemod.2018.05.002

Zhang, S., Curchitser, E. N., Kang, D., Stock, C. A., & Dussin, R. (2018). Impacts of mesoscale eddies on the vertical nitrate flux in the Gulf Stream region. *Journal of Geophysical Research: Oceans*, *123*, 497–513. https://doi.org/10.1002/2017JC013402

Zhang, W. G., & Gawarkiewicz, G. G. (2015). Dynamics of the direct intrusion of Gulf Stream ring water onto the Mid-Atlantic Bight shelf. *Geophysical Research Letters*, *42*, 7687–7695. https://doi.org/10.1002/2015GL065530

Zhang, W. G., McGillicuddy, D. J., & Gawarkiewicz, G. G. (2013). Is biological productivity enhanced at the New England shelfbreak front? *Journal of Geophysical Research: Oceans*, *118*, 517–535. https://doi.org/10.1002/jgrc.20068